Effects of antenatal corticosteroid treatment on immune cell development and seeding of secondary lymphoid organs in the offspring

Dissertation

zur Erlangung des akademischen Grades einer
Doktorin der Medizin (Dr. med.)

an der

Medizinischen Fakultät der Universität Hamburg

vorgelegt von

Elena Billeb

aus

München

2025

Betreuer:in / Gutachter:in der Dissertation: Prof. Dr. Eva Tolosa

Gutachter:in der Dissertation: Prof. Dr. Samuel Huber

Vorsitz der Prüfungskommission: Prof. Dr. Samuel Huber

Mitglied der Prüfungskommission: Prof. Dr. Madeleine Bunders

Mitglied der Prüfungskommission: Prof. Dr. Hans-Willi Mittrücker

Datum der mündlichen Prüfung: 21.11.2025

Table of contents

1. Aims of this thesis

Antenatal corticosteroids (ACS) are routinely administered to women at risk of preterm delivery to promote fetal lung maturation. While the benefits of ACS in reducing the incidence of acute respiratory distress syndrome (ARDS) are well-established, prenatal steroid exposure also induces apoptosis in developing T cells (Wyllie, 1980; Taves and Ashwell, 2021) and causes thymic atrophy (Diepenbruck *et al.*, 2013; Jones *et al.*, 2020), raising concerns about broader immunological consequences. Given the potent immunomodulatory properties of glucocorticoids, it has been suggested that prenatal exposure may result in significant alterations in neonatal immune cell development and function. However, the specific consequences of steroid-induced lymphopenia on the development and seeding of immune cells to the periphery remain unknown.

We hypothesize that prenatal corticosteroid exposure induces transient lymphopenia, thereby delaying the migration of immune cells to peripheral lymphoid organs (Figure 1). Such altered immune cell dynamics may influence antiviral immune responses.

To address this hypothesis, we used a previously established mouse model of prenatal corticosteroid treatment and performed comprehensive immunophenotyping of central and peripheral immune compartments in the offspring. In addition, a neonatal murine cytomegalovirus (MCMV) infection model was used to evaluate whether steroid-induced immune alterations affect antiviral immune responses.

Accordingly, the aims of this thesis are:

- To investigate the impact of prenatal corticosteroid exposure on lymphoid progenitors and the migration of immune cells to the periphery using a pregnancy mouse model.
- To evaluate the neonatal immune response to MCMV infection following perinatal exposure to betamethasone.

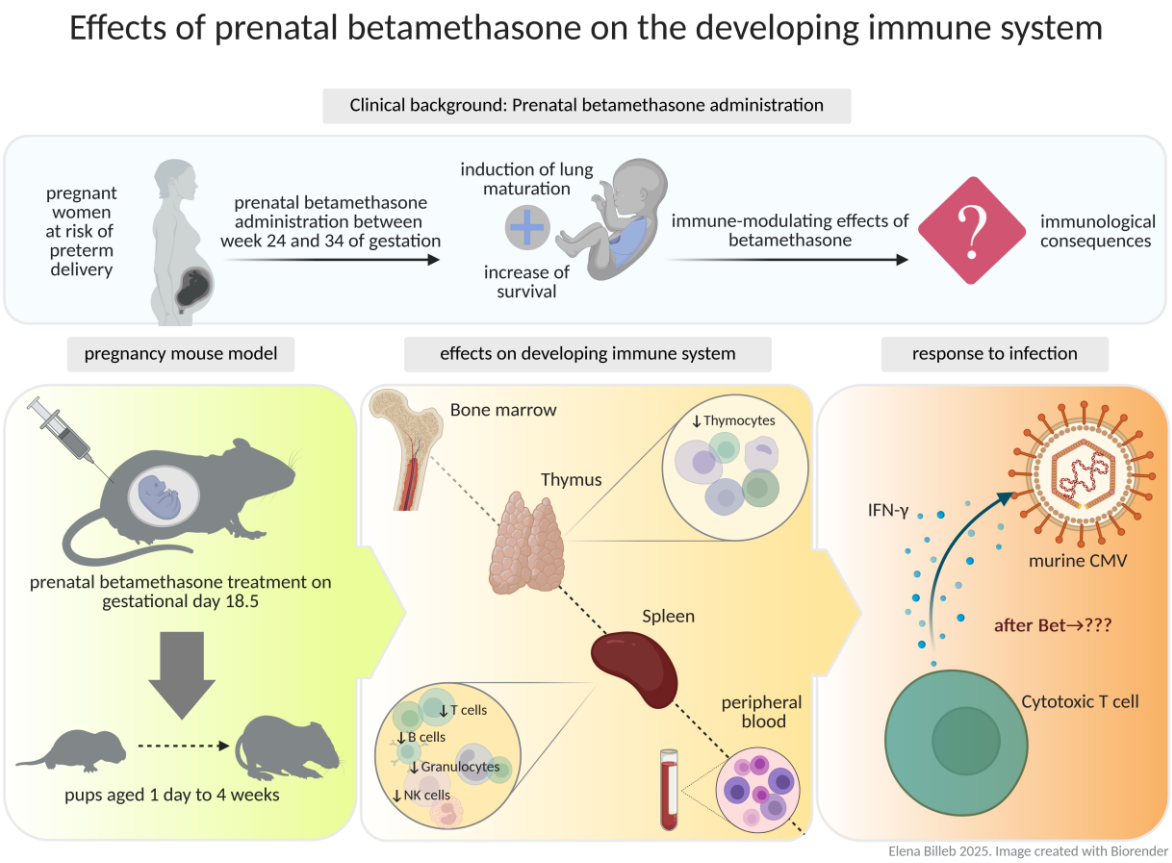

Figure 1: Graphical abstract. Prenatal betamethasone is administered to pregnant women at risk of preterm delivery. The specific immunomodulatory effects of prenatal betamethasone in the neonates remain poorly understood. To investigate this, immunophenotyping of central and peripheral immune compartments was conducted in a pregnancy mouse model, alongside neonatal MCMV infection to assess functional consequences.

2. Introduction

2.1. Hematopoiesis and immune cell development

The immune system is a complex network of cells and their secreted products that is crucial for the protection from pathogens and potentially harmful substances. To ensure proper functioning, a delicate balance between sensitivity towards pathogens and self-tolerance must be established during early hematopoietic development.

In mammals, two waves of “primitive” hematopoietic cells are produced in early embryological development in the extraembryonic yolk sac (YS), allantois and placenta. Erythroid-myeloid progenitors (EMPs) give rise to embryonic, nucleated erythrocytes, macrophages and blood platelets and lack lymphopoietic abilities (Palis *et al.*, 1999). They are later replaced by definitive hematopoietic cells, although murine data suggests that erythropoiesis from YS EMPs continues until birth (Chen *et al.*, 2011; Palis, 2014; McGrath

et al., 2015). Interestingly, yolk sac-derived tissue resident macrophages can persist into adulthood (Gomez Perdiguero *et al.*, 2015; Soares-da-Silva *et al.*, 2023). The first pluripotent repopulating hematopoietic stem cells (HSCs) with lymphoid potential mainly emerge from the aorta-gonad-mesonephros region (Müller *et al.*, 1994; de Bruijn *et al.*, 2000) – a potent hematopoietic site within the mammalian embryo body - around gestational day 30 in humans and day E10.5 in mice (Medvinsky and Dzierzak, 1996; Kumaravelu *et al.*, 2002; Ivanovs *et al.*, 2011). HSCs then migrate to the fetal liver, where they expand and generate the first wave of leukocytes (Dzierzak and Speck, 2008) and start colonizing thymus and spleen (Haynes and Heinly, 1995). During the second trimester of pregnancy in humans (Holt and Jones, 2000) and shortly before birth in mice, HSCs leave the fetal liver and move to bone marrow, which becomes the major site of leukopoiesis (Christensen *et al.*, 2004; Rieger and Schroeder, 2012; Soares-da-Silva *et al.*, 2020). Importantly, fetal liver remains the main site of leukopoiesis in mice until birth (Hall *et al.*, 2022). Table 1 summarizes the key time points of prenatal hematopoiesis in mice and humans.

Table 1: Comparison of relevant time points in early hematopoiesis in mice and humans. Time points describe first appearance of hematopoietic stem or progenitor cells in embryonic tissues and fetal organs. AGM = aorta-gonad-mesonephros region EMP = erythroid-myeloid progenitors, E = embryonic day, PCW = postconceptual week.

First appearance of hematopoietic (stem) cells in embryonic tissues and fetal organs							
Species	Yolk sac	AGM region	Fetal liver	Thymus	Spleen	Bone Marrow	Duration of pregnancy
Mice	E7.5-E9.5	E9.5-E11	E11.5-E16.5	E11	E15.5	*E14.5-E17.5 **	19-21 days
Human	2-3 PCW	4 PCW	6 PCW	8-9 PCW		10 PCW	38 PCW
	Primitive blood cells, EMPs	*First HSCs with lymphoid potential*	*HSC expansion*			** minimal activity until birth*	

The hematopoietic stem cell niche in bone marrow is maintained by cytokine signaling via stem cell factor (SCF) and CXCL12 and their respective receptors cKit (CD117) and CXCR4 (Ding *et al.*, 2012). Progenitor cell proliferation and differentiation is driven by activation of receptor tyrosine kinase FLT3 by FLT3L in synergy with other cytokines such as SCF, IL-3, IL-6, Granulocyte-Macrophage Colony stimulating Factor (GM-CSF),

Granulocyte Colony Stimulating Factor (G-CSF) and IL-11 (Banu *et al.*, 1999; Tsapogas *et al.*, 2017). HSCs gradually loose stem cell potential and develop into multipotent progenitors (MPPs). MPPs begin expressing lineage-determining transcription factors that drive further differentiation into the different hematopoietic cell lines (Figure 2). Expression of transcription factor GATA1 promotes differentiation of MPPs to megakaryocyte-erythrocyte-progenitors (MEP), which are responsible for erythrocyte and blood platelet development (Korzhenevich *et al.*, 2023). Transcription factors CCAAT/Enhancer Binding protein alpha (C/EBPα) and PU.1 promote development into common myeloid progenitors (CMP) and subsequently give rise to granulocyte-macrophage progenitors (GMPs) that differentiate into either granulocytes (eosinophils, neutrophils and basophils), or macrophage and dendritic cell (DC) progenitors (MDPs). MDPs can develop into monocytes or common dendritic cell progenitors (CDPs) that mature into dendritic cells, although certain DC subsets also derive from common lymphoid progenitors (CLPs) (Geissmann *et al.*, 2010; Rieger and Schroeder, 2012). A downregulation of C/EBPα in MPPs by transcription factor Early B-Cell Factor 1 (EBF1) drives differentiation into lymphoid-primed MPPs (LMPP) (Rieger and Schroeder, 2012; Lenaerts *et al.*, 2022).

Driven by activation of tyrosine kinase FLT3 (CD135), LMPPs develop into CLPs and upregulate *E2a, IL7-RA* and Early B cell factor *EBF1* (Boller and Grosschedl, 2014). CLPs differentiate into innate lymphoid cells (ILCs) including natural killer cells (NK cells) (Zook and Kee, 2016), T cell committed progenitors (TLPs) or B cell committed progenitors (BLPs (Rieger and Schroeder, 2012). While paired box 5 (PAX5) promotes B cell lineage, Notch1 expression results in T cell commitment (Souabni *et al.*, 2002; Schmitt *et al.*, 2004; Tagoh *et al.*, 2006; Nutt and Kee, 2007). In adult, *i.e.* post-embryonic lymphopoiesis, BLPs remain in bone marrow to develop into mature B cells while T cell-committed progenitors migrate to the thymus and are subsequently called thymus seeding progenitors (TSP).

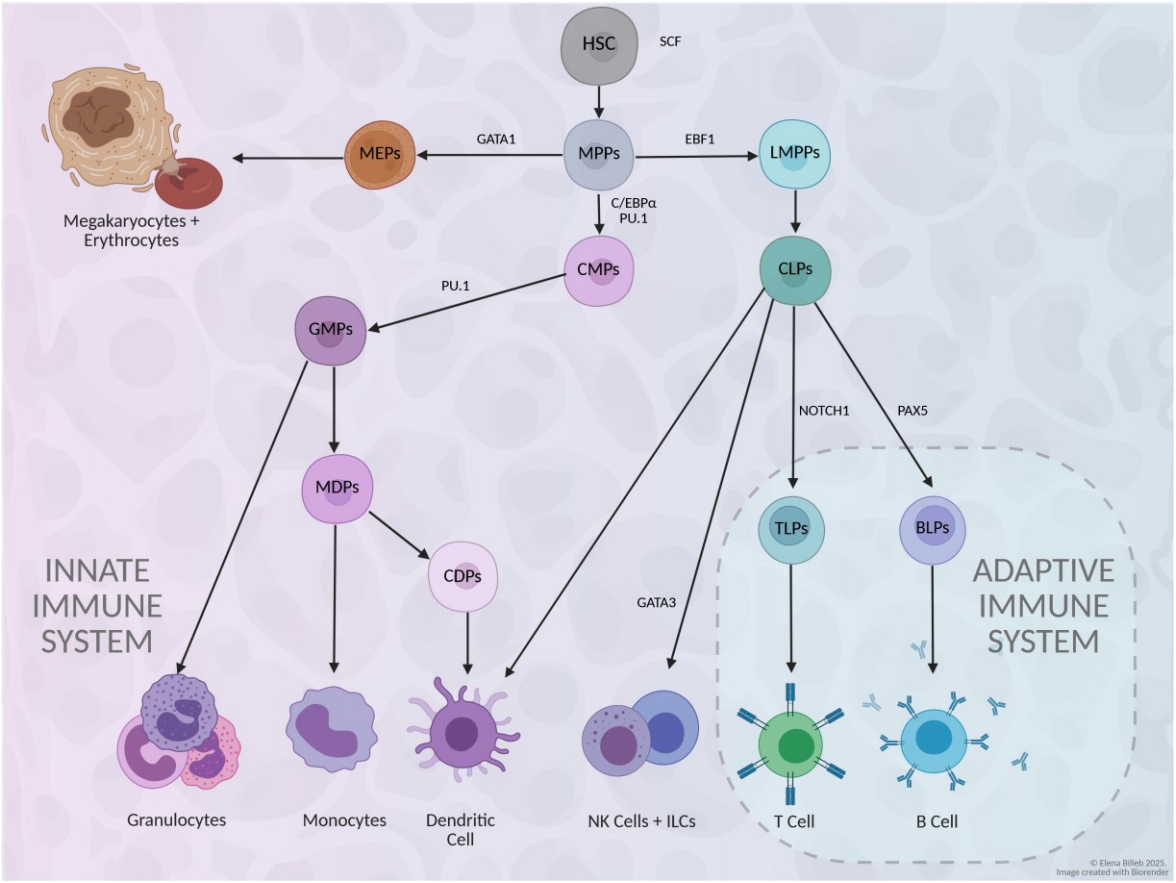

Figure 2: Immune cell development. Hematopoietic stem cells (HSCs) differentiate into multipotent progenitors (MPPs), which give rise to erythroid, myeloid, or lymphoid lineages. Myeloid differentiation proceeds via common myeloid progenitors (CMPs), while lymphoid-primed MPPs (LMPPs) generate common lymphoid progenitors (CLPs) that give rise to B cells, T cells, and innate lymphoid cells, including NK cells. HSC = Hematopoietic stem cell, MPP = Multipotent progenitor cell, MEP = megakaryocyte-erythrocyte-progenitor cell, LMPP = lymphoid-primed MPP, CMP = common myeloid progenitor cell, GMP = Granulocyte-macrophage-progenitor, CDP = common dendritic cell progenitor, MDP = Monocyte-dendritic cell progenitor, CLP = Common lymphoid progenitor, TLP = T-cell committed lymphoid progenitor, BLP = B-cell committed lymphoid progenitor.

2.1.1. T cell development

T cells are a crucial part of the adaptive immune system that mediate immune responses by recognizing specific antigens through their T cell receptors.

Early T cell development is driven by interaction of Notch1 on thymocytes with respective ligands like Jagged 1 and Jagged 2 on thymic stromal cells (Robson MacDonald, Wilson and Radtke, 2001). Thymus-seeding progenitors (TSPs) enter the thymus at the corticomedullar junction (CMJ) (Zúñiga-Pflücker, 2004). At that early stage, they lack expression of CD4 and CD8 and are defined as double negative (DN) thymocytes (Figure 3). DNs migrate through the thymic outer cortex, and differentiate from $CD25^{-}$ $CD44^{+}$ DN1 into $CD25^{+}$ $CD44^{+}$ DN2,

$CD25^+$ $CD44^+$ DN3 and finally $CD25^-$ $CD44^-$ DN4 cells. At the DN2 stage, thymocytes begin development of the T-cell receptor (TCR) by rearrangement of V and J gene segments for the TCRβ chain, determining their fate as conventional αβT cells, while γδT cell progenitors follow an alternative developmental pathway from DN or ISP8 stages. Together with a surrogate TCRα chain, β-selected DN 3 cells now express a pre-TCR (von Boehmer *et al.*, 1998; Bosselut and Vacchio, 2016). After subsequent upregulation of CD8, murine thymocytes enter an intermediate single positive stage (ISP8 cells), marking the start of the TCRα-chain rearrangement. If successful, thymocytes now express a complete TCRαβ and differentiate into $CD8^+$ $CD4^+$ double positive (DP) thymocytes. DPs are positively selected based on their TCR-binding ability to major histocompatibility complex (MHC) molecules on cortical thymic epithelial cells. While thymocytes with low to no binding affinity are neglected, positively selected thymocytes receive positive survival signals via their TCR and enter the thymic medullary region (Jameson, Hogquist and Bevan, 1995). In a second selection process called negative selection or central tolerance, thymocytes that have entered the thymic medulla are challenged with endogenous peptides presented by medullary thymic epithelial cells (mTECs). Thymocytes that bind these peptides with high affinity are reprogrammed into regulatory T cells (agonist selection) or undergo apoptosis and are thereby negatively selected, whereas those with low to intermediate binding strength survive. Thymocytes mature into $CD4^+$ single positive T helper cells that recognize antigen presented by MHC class II molecules or $CD8^+$ single positive cytotoxic T cells with binding ability to MHC class I receptors and migrate into the periphery (Figure 3). Both selection processes together ensure functioning T cells that recognize pathogens while also maintaining self-tolerance (Palmer, 2003; Hogquist, Baldwin and Jameson, 2005; Miller, 2011).

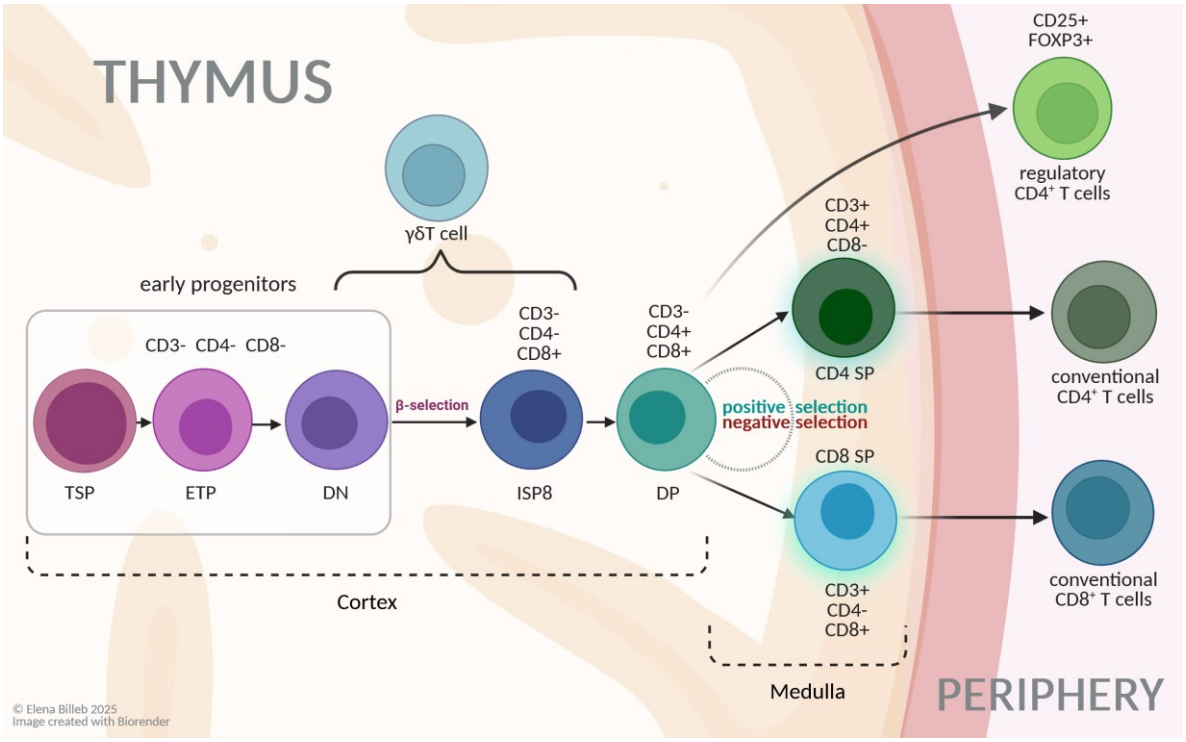

Figure 3: Murine T cell development. Thymus-seeding progenitors (TSPs) enter the thymus at the corticomedullary junction and progress through defined double negative (DN) stages before becoming double positive (DP) thymocytes, which are positively selected in the cortex based on their ability to bind MHC molecules. Positively selected cells migrate to the medulla, where negative selection eliminates thymocytes with high-affinity binding to self-antigens, ensuring the development of functional, self-tolerant CD4 or CD8 single positive T cells. TSP = Thymus-seeding progenitor, ETP = Early thymus progenitor, DN = Double negative thymocyte, ISP8 = intermediate CD8 single positive thymocyte, DP = Double positive thymocyte: CD4SP = CD4 single positive T-cell, CD8SP SP = CD8 single positive T cell.

2.2.2. B cell development

B cells express unique B cell receptors (BCRs) and play a central role in mediating humoral immune responses. Upon activation by T cells or antigen-presenting cells, B cells differentiate into plasma cells and produce antigen-specific antibodies.

B cell-committed progenitors remain in bone marrow and develop into fully functional, immature B cells (Figure 4), starting as (early) Pro-B cells. E2A and EBF1 promote the expression of recombination activation genes *RAG-1* and *RAG-2* which induce the rearrangement of V(D)J-gene segments for the immunoglobulin heavy chain (IgH). When rearranged successfully, IgH is expressed as μ-chain together with a surrogate IgL chain, forming the pre-B cell receptor (pre-BCR) (Korzhenevich *et al.*, 2023). Cells that fail to generate a IgH are neglected, while those expressing pre-BCR receive IL-7 mediated survival signals and undergo clonal expansion. Pre-B cells then exit the cell cycle and begin VJ

recombination of the light chain (L-chain). Successfully rearranged L-chains form IgM molecules together with µ-chains, leading to development of Pre-B cells into immature B cells. Based on the BCR-signal strength following antigen presentation, immature B cells are either positively selected or continue rearrangement of the L-chain. Cells with high affinity to self-antigen are negatively selected and repeat IgL-rearrangement (receptor editing) or undergo apoptosis (clonal deletion). Non-autoreactive B cells migrate to spleen where they finally differentiate into marginal zone or follicular B cells (Berek, Radbruch and Schroeder, 2008; Nemazee, 2017; Korzhenevich *et al.*, 2023).

After maturation, T and B cells populate the secondary lymphoid organs and blood, forming the basis of adaptive immunity (Bonilla and Oettgen, 2010).

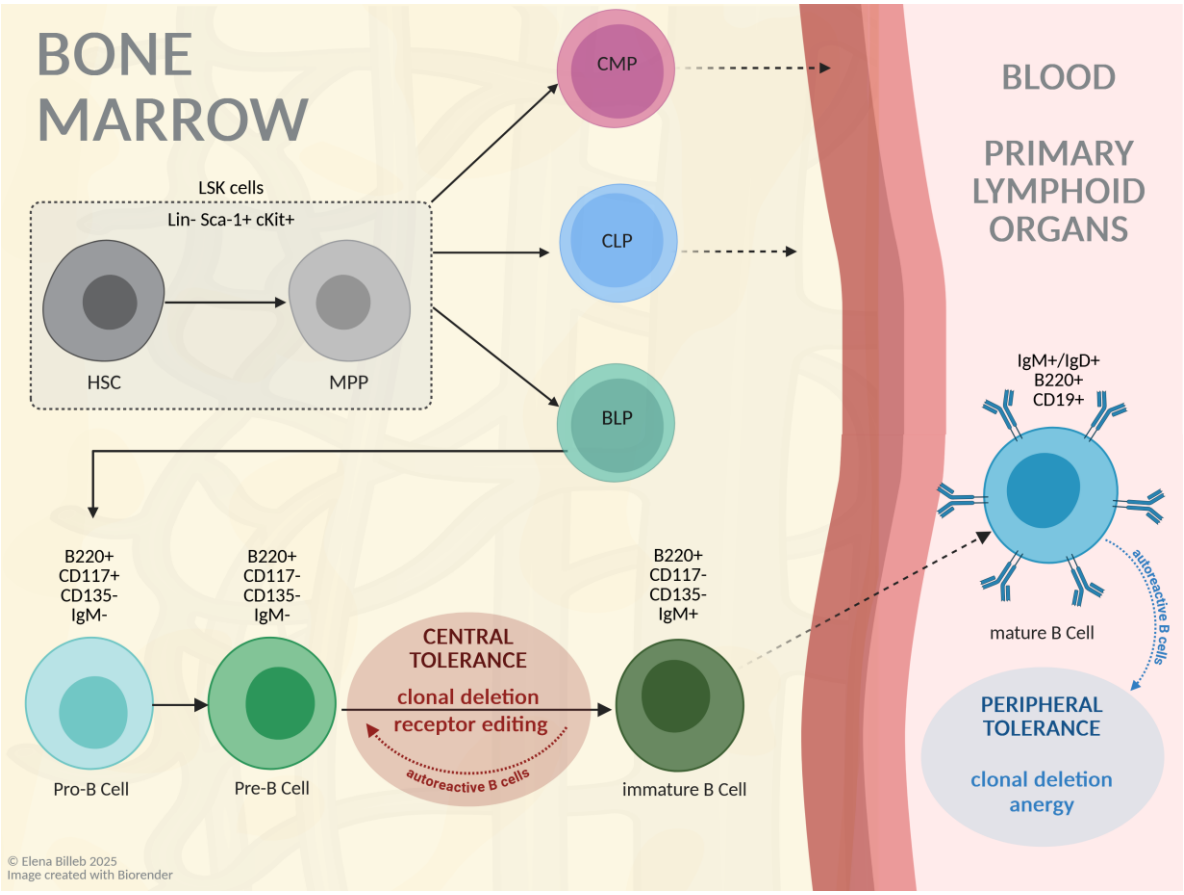

Figure 4: Murine B cell development. B cell-committed progenitors (BLP) undergo immunoglobulin gene rearrangements to form a functional B cell receptor (BCR) and undergo different maturation steps from Pro-B cells to Pre-B cells and finally IgM-expressing immature B cells that migrate to spleen.

2.2. Neonatal infections

Neonatal infections are one of the major challenges of newborn children, especially in preterm infants. The most common and serious neonatal infection is neonatal sepsis, defined as a systemic, potentially life-threatening infection in the neonatal period mainly caused by bacteria or, less frequently, fungi (Shah and Padbury, 2014). Depending on the time point of infection, neonatal sepsis is further classified into early-onset sepsis that occurs within the first 72 hours of life and is mostly caused by vertical infections during birth, and late-onset sepsis, occurring after 72 hours of life by community-acquired and nosocomial infections (Camacho-Gonzalez, Spearman and Stoll, 2013). Immune responses to bacterial infections are mainly mediated by innate immune cells like neutrophils and monocytes. During the perinatal period and especially in preterm infants, the function and quantity of neutrophils is still insufficient, making these children particularly susceptible to severe bacterial infections (Melvan *et al.*, 2010; Zhang, Zhivaki and Lo-Man, 2017).

Although bacterial infections present an acute risk for newborn infants, they are not the only infectious threat in the neonatal period. While neonatal care progresses and survival improves (Perin *et al.*, 2022), nosocomial infections and viral pathogens remain persistent challenges (Raymond and Aujard, 2000; Tabone *et al.*, 2000; Zaoutis *et al.*, 2006; Preidis *et al.*, 2011; Bateman *et al.*, 2021). Lower respiratory infections account for 8.3 % of deaths below the age of 1 month and 13.9 % below the age of 5 years (Perin *et al.*, 2022). One of the leading causes remains respiratory syncytial virus (RSV), posing a threat especially in the first year of age, in children with underlying medical conditions and in premature infants (Stein *et al.*, 2017). Moreover, perinatal viral infections, in particular with cytomegalovirus (CMV), account for a majority of live-altering CNS infections in otherwise healthy neonates (Abeywickrema, Kelly and Kadambari, 2023).

Human cytomegalovirus (HCMV) is a pathogen also known as human herpes virus 5 (Arvin *et al.*, 2007). Like many viral infections, the elimination of CMV is predominantly initiated by T cell mediated immune responses (Klenerman and Oxenius, 2016; Fonseca Brito, Brune and Stahl, 2019). Cytotoxic $CD8^+$ T cells and, to a lesser extent, $CD4^+$ T cells recognize CMV antigens presented by antigen presenting cells (APCs) and initiate an inflammatory cascade by producing IFNγ and other pro-inflammatory cytokines (Fonseca Brito, Brune and Stahl, 2019). Congenital CMV infection (cCMV) occurs in around 0,6 % of all births with around 11 % symptomatic infants at time of delivery (Kenneson and Cannon, 2007). cCMV can cause

severe neurologic damage and is one of the main causes for sensorineural hearing loss in small children (Grosse, Ross and Dollard, 2008; Palmetti *et al.*, 2025). Furthermore, it can result in severe neurological and neurodevelopmental sequelae including microcephaly and cerebellar hypoplasia, intracerebral calcifications and chorioretinitis (Swanson *et al.*, 2025). Postnatal CMV infection is often asymptomatic in immunocompetent children and adults, but it can result in increased morbidity and severe outcomes in immunodeficient and premature children (Osterholm and Schleiss, 2020; Bateman *et al.*, 2021).

2.3. Prenatal steroids

Since its introduction in the 1970s, antenatal corticosteroid (ACS) treatment drastically reduced morbidity and mortality in preterm infants (Liggins and Howie, 1972). Pregnant women at risk of preterm delivery receive betamethasone or dexamethasone between gestational weeks 24 and 34 (Dagklis *et al.*, 2022). Within 24 hours, the steroid induces fetal lung maturation by stimulating surfactant production, leading to a significant reduction in mortality by decreasing the risk of respiratory distress syndrome in preterm infants (McGoldrick *et al.*, 2020).

Glucocorticoids (GCs) are steroid hormones with broad functions in development, growth and homeostasis (Oppong and Cato, 2015). GCs bind cytosolic glucocorticoid receptors (GRs) that translocate to the cell nucleus, where they function as transcription factor (TF) or TF modulators for a variety of genes, and for instance induce a negative regulation of pro-inflammatory genes such as *AP-1* and *NF-κB* (Jonat *et al.*, 1990; Scheinman *et al.*, 1995; Kumar and Thompson, 2005). Endogenous GCs produced by thymic epithelial cells (TECs) are important for mediating of thymocyte survival during selection processes in thymus (Vacchio, Papadopoulos and Ashwell, 1994; Tolosa, King and Ashwell, 1998; Mittelstadt, Taves and Ashwell, 2018; Taves and Ashwell, 2021). In pregnancy, 11β-hydroxysteroid dehydrogenase type 2 (11β-HSD2), a glucocorticoid inactivating enzyme, is expressed at the feto-placental barrier and protects the offspring from excessive steroid exposure (Benediktsson *et al.*, 1997; Solano *et al.*, 2016). Free endogenous GCs are mainly bound by corticosterone-binding globulin (CBG), while synthetic GCs show a low affinity to CBG and are either bound to albumin or remain unbound in maternal plasma. In elevated concentrations, both endogenous and synthetic glucocorticoids can lead to an oversaturation of corticosteroid binding proteins and functional exhaustion of 11β-HSD2,

leading to elevated levels of free GCs that pass the placenta-fetal barrier and bind to fetal GRs (Kajantie *et al.*, 2004; Mattos *et al.*, 2013). Severe maternal psychological distress leads to elevated endogenous (maternal) glucocorticoid levels and is associated with an increase of atopic dermatitis and childhood asthma in the offspring (Fang *et al.*, 2011; Wen *et al.*, 2011; Larsen *et al.*, 2014; Chang *et al.*, 2016; Lee *et al.*, 2016). Moreover, one study reported an increased occurrence of lymphatic and testicular cancer in children if mothers experienced grieve during pregnancy (Lorenzo Bermejo, Sundquist and Hemminki, 2007). Prenatally administered synthetic GCs, besides their clearly established benefits for lung development in preterm infants, are also highly immunomodulatory drugs with the capacity to induce apoptosis in both developing and mature T (Wyllie, 1980; Taves and Ashwell, 2021) and B cells (Lill-Elghanian *et al.*, 2002; Gruver-Yates, Quinn and Cidlowski, 2013) and result in reduced thymic volumes in mice (Diepenbruck *et al.*, 2013) as well as in humans (Jones *et al.*, 2020). Prenatal corticosteroid exposure induces apoptosis of developing murine thymocytes, especially $CD4^+$ $CD8^+$ double positive thymocytes (Diepenbruck *et al.*, 2013; Gieras *et al.*, 2017; Perna-Barrull *et al.*, 2019), but also in human CD4 single positive T cells (Chabra *et al.*, 1998). Prenatal dexamethasone exposure results in long-lasting impairment of murine CD8 T cell functions (Hong *et al.*, 2020). In mice, prenatal betamethasone leads to changes in the T cell receptor repertoire that potentially increase the risk for developing autoimmune diseases like systemic lupus erythematosus but seem to have a protective effect regarding type 1 diabetes (Gieras *et al.*, 2017; Perna-Barrull *et al.*, 2019). Epidemiologically, ACS administration is associated with higher susceptibility to allergic diseases such as asthma and allergic rhinitis (Pole *et al.*, 2009; Tseng *et al.*, 2016). Taken together, prenatally administered glucocorticoids may impact the immunological profile of the progeny.

3. Material and Methods

3.1. Material

3.1.1. Mouse strains

Strain	Source	Animal ethics
C57BL/6J	University Medical Center Hamburg-Eppendorf (UKE)	N19/094

3.1.2. Reagents and solutions

Material	Company
Betamethasone	Sigma-Aldrich, St. Louis (MO), USA
Dulbecco's Phophate Buffered Saline (PBS)	Thermo Fisher Scientific, Waltham (MA), USA
Ethanol	Roth, Karlsruhe, Germany
Live/Dead Dye Pacific Orange Succininidyl Ester	Invitrogen, Carlsbad (CA), USA
eBioscience™ 10x RBC Lysis Buffer	Invitrogen, Carlsbad (CA), USA
Phorbol-12-myristat-13-acetat	Sigma-Aldrich, St. Louis (MO), USA
Ionomycin	Sigma-Aldrich, St. Louis (MO), USA
X vivo medium	Lonza, Basel, Switzerland

3.1.3. Buffer and media

Buffer	Composition
Annexin buffer	H_20 with 1.4 M NaCl 25 mM CaCl2 0.1 M Hepes
FACS buffer	PBS with +0.1 % BSA +0.02 % NaN3
Cell Counting Medium	RPMI with + 10 % FBS

3.1.4. Kits

Kit	Company
eBioscience™ Anti-human FoxP3 Staining Set APC	Invitrogen, Carlsbad (CA), USA

3.1.5. Flow cytometry antibodies

specificity	fluorochrome	clone	company	panel
Annexin V	FITC	-	Becton Dickinson, Franklin Lakes (NJ), USA	2
B220	BV480	RA3-6B2	Becton Dickinson, Franklin Lakes (NJ), USA	4
B220	BV785	RA3-6B2	BioLegend, San Diego (CA), USA	1
CCR6	AF647	11A9	Becton Dickinson, Franklin Lakes (NJ), USA	3
CD117	PerCPCy5.5	2B8	BioLegend, San Diego (CA), USA	1,2
CD11b	FITC	M1/70	BioLegend, San Diego (CA), USA	3
CD11b	Pe-Cy7	M1/70	BioLegend, San Diego (CA), USA	1
CD11c	BV421	N418	BioLegend, San Diego (CA), USA	3
CD127	BV421	A7R34	BioLegend, San Diego (CA), USA	3
CD127	PE-CF594	SB/199	Becton Dickinson, Franklin Lakes (NJ), USA	4
CD135	BV421	A2F10	BioLegend, San Diego (CA), USA	1
CD19	PE-Cy7	1D3	eBioscience, San Diego (CA), USA	3
CD25	BV650	PC61	BioLegend, San Diego (CA), USA	3
CD25	BV421	PC61	BioLegend, San Diego (CA), USA	2
CD25	BV421	PC61	Biolegend, San Diego (CA), USA	4
CD27	PE	I.G.3A10	BioLegend, San Diego (CA), USA	2
CD3	PE	145-2C11	BioLegend, San Diego (CA), USA	3
CD3	PECy7	145-2C11	BioLegend, San Diego (CA), USA	1,2
CD4	PerCP	RM4-5	BioLegend, San Diego (CA), USA	3
CD4	AF700	RM4-5	BioLegend, San Diego (CA), USA	2
CD4	R718	RM4-5	Becton Dickinson, Franklin Lakes (NJ), USA	4
CD44	APC-Cy7	IM7	BioLegend, San Diego (CA), USA	2
CD44	FITC	IM7	BioLegend, San Diego (CA), USA	4
CD45	AF700	30-F11	BioLegend, San Diego (CA), USA	3
CD45	APC-Cy7	30-F11	BioLegend, San Diego (CA), USA	1
CD45	PE-Cy7	30-F11	Biolegend, San Diego (CA), USA	4
CD48	AF-700	HM48-1	BioLegend, San Diego (CA), USA	1
CD49d	BV786	R1-2	Becton Dickinson, Franklin Lakes (NJ), USA	4
CD69	BV785	H1.2F3	BioLegend, San Diego (CA), USA	2

CD8a	APC-Cy7	53-6.7	BioLegend, San Diego (CA), USA	3
CD8a	BV650	53-6.7	BioLegend, San Diego (CA), USA	2, 4
Gr-1	Pe-Cy7	RB6-865	BioLegend, San Diego (CA), USA	1
IgM	PE	RMM-1	BioLegend, San Diego (CA), USA	1
Ly6D	FITC	49-H4	BioLegend, San Diego (CA), USA	1
Ly6G	PerCPCy5.5	1A8	Becton Dickinson, Franklin Lakes (NJ), USA	3
MHCII	BV785	M5/114.15.2	BioLegend, San Diego (CA), USA	3
NK1.1	PE-Cy7	PK136	BioLegend, San Diego (CA), USA	3
Sca-1	APC	D7	BioLegend, San Diego (CA), USA	1
TCRβ	BV605	H57-597	BioLegend, San Diego (CA), USA	2
TCRβ	PerCPCy5.5	H57-597	BioLegend, San Diego (CA), USA	4
TCRγδ	BV605	GL3	BioLegend, San Diego (CA), USA	3, 4
TCRγδ	APC	eBioGL3	Thermo Fisher Scientific, Waltham (MA), USA	2
KLRG1	APC-Cy7	2F1/KLRG1	BioLegend, San Diego (CA), USA	4
IFN-γ	PE	XMG1.2	BioLegend, San Diego (CA), USA	4

3.1.6. Equipment

Equipment	Company, Location
Analytical balance LA 124i	VWR International, Radnor (PA), USA
BMP51 Label Printer Cartridge	Brady Corporation, Milwaukee (WI), USA
Centrifuge 5810R	Eppendorf, Hamburg, Germany
Centrifuge Allegra X-30R	Beckmann Coulter, Brea (CA), USA
Eppendorf-Multipette M4	Eppendorf, Hamburg, Germany
FACS Celesta	Becton Dickinson, Franklin Lakes (NJ), USA
FACSymphony A1	Becton Dickinson, Franklin Lakes (NJ), USA
Label Printer BMP51	Brady Corporation, Milwaukee (WI), USA
NucleoCounter® NC-200	Chemometec, Allerod, Denmark
Pipettes 2.5/10/20/200/1000 µL	Eppendorf, Hamburg, Germany
Pipettes 200/1000 µL	Gilson Incorporated, Middleton (WI), USA
Refrigerator/Freezer	Liebherr, Bulle, Switzerland

ScanLaf Class 2 Biological safety cabinet MARS	LaboGene, Lillerød, Dänemark
Sterile cabinet MSC-Advantage 1.8	Thermo Fisher Scientific, Waltham (MA), USA
Via1-Cassette™	Chemometec, Allerod, Denmark
Vortex mixer Gene 2	Scientific industries, Bohemia (NY), USA

3.1.7. Consumables

Consumables	Company, Location
Pipette tips 10/200/1000 µL	Sarstedt, Numbrecht, Germany
epT.I.P.S 10/200/1000 µL	Eppendorf, Hamburg, Germany
FALCON® 70 µm Nylon cell strainer	Corning, Amsterdam, Netherlands
B|BRAUN Omnifix-Tuberculin syringes 1 mL	B. Braun, Hessen, Germany
Stericain B|BRAUN injection needles 27 G x 3/4	B. Braun, Hessen, Germany
SafeSeal tubes 1.5/2 mL	Sarstedt, Numbrecht, Germany
Polystyrene round bottom tubes 5 mL	Sarstedt, Numbrecht, Germany
Cellstar polypropylene tubes 15/50 mL	Greiner bio-one, Kremsmunster, Austria
Microtubes K3E 1.3 mL 1.6 mg EDTA/mL	Sarstedt, Numbrecht, Germany
TruCount™ Tubes 5 mL	Becton Dickinson, Franklin Lakes (NJ), USA

3.1.8. Software

Software	Company, Location
FACSDivaTM V.8.0.1	Becton Dickinson, Franklin Lakes (NJ), USA
FlowJo V10 10.5.3	FlowJo, LLC, Ashland, USA
GraphPad Prism 10	GraphPad Software, Inc., La Jolla, USA
BioRender: Scientific Image and Illustration Software	BioRender Toronto (ON), Canada

3.1.9. AI-based tools

Tool	Purpose	Section(s)
ChatGPT (chat.openai.com)	language correction of the first draft	Introduction and work hypothesis

3.2. Methods

3.2.1. Murine experiments

3.2.1.1. Prenatal steroid mouse model

C57BL/6JWT mice were purchased from the local animal breeding-facility of the University Medical Center Hamburg-Eppendorf and housed and maintained under pathogen-free conditions. Mice received food and water *ad libitum.* C57BL/6JWT dams and males were mated and the presence of a vaginal plug considered as day 0.5 of pregnancy (E 0.5). 0.1 mg betamethasone (Sigma-Aldrich, Germany) or vehicle control (PBS) was administered intraperitoneally to pregnant dams on day E 18.5 (Figure 5). Overall health and animal weights were scored over the course of maximal four weeks, after which animals were sacrificed according to institutional guidelines for organ harvesting.

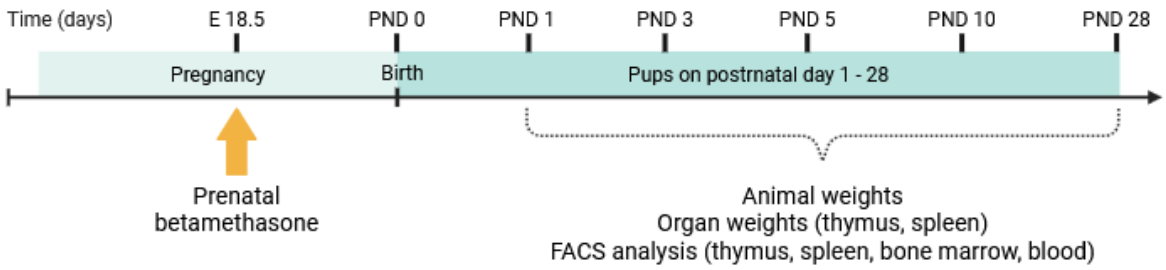

Figure 5: Schematic illustration of the ACS treatment pregnancy mouse model. 0.1 mg betamethasone was administered to the pregnant dams on E 18.5, and neonatal bone marrow, thymus, spleen and blood subsequently collected from newborn pups between PND 1-28. Pup and organ weights were acquired, followed by immune phenotyping of tissue samples using flow cytometry.

3.2.1.2. MCMV infection mouse model

C57BL/6 wildtype were mated and dams were kept with their litter. Neonatal mice received 0.06 µg betamethasone (Sigma-Aldrich, Germany) or vehicle control (PBS) subcutaneously

on their first day of life. All pups were infected intratracheally with 104 plaque-forming units (PFU)/mL MCMV-2DR on postnatal day (PND) 0. After 14 days, pups were sacrificed and blood, salivary glands, lungs, spleens and livers collected for examination of viral loads and immune phenotyping (Figure 6). For intratracheal inoculations, a volume of 10 µl was administered by probing of the laryngopharynx with a pipette and extension of the neck. MCMV-2DR has been described previously (Bošnjak *et al.*, 2023) and was produced and titrated on mouse 10.1 and M2-10B4 fibroblasts, respectively. MCMV-2DR encodes Gaussia luciferase and mCherry and the full-length MCMV m129. The reporter virus lacks the m157 ORF that encodes a ligand for the activating receptor Ly49H present on NK cells in C57BL/6 mice. Infections and infection readouts were performed in the laboratory AG Stahl by F. Stahl, S. Tödter and L. Fonseca Brito.

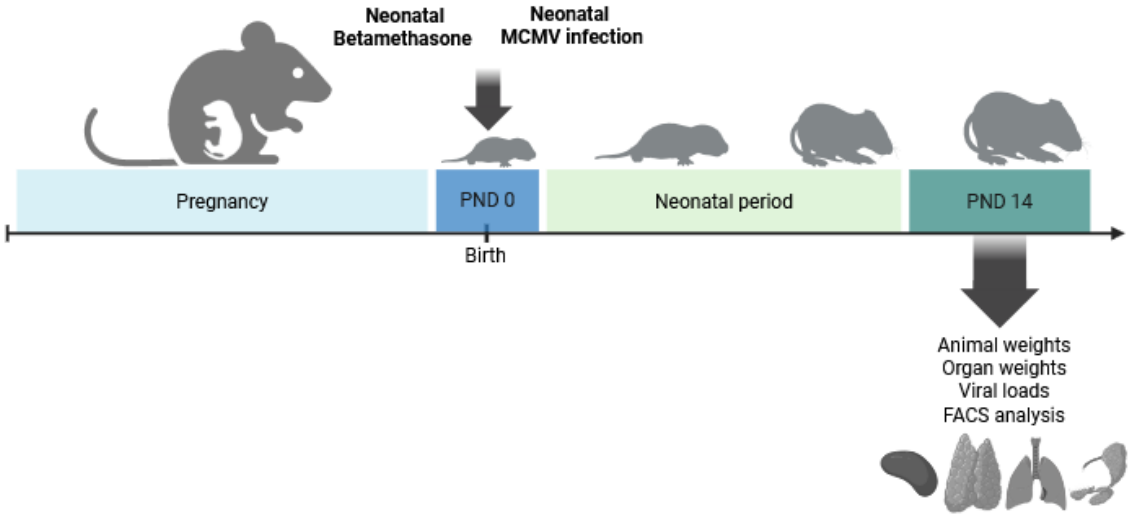

Figure 6: Schematic illustration of the MCMV infection mouse model. 0.6 µg betamethasone or PBS vehicle control was administered directly to the pups immediately after birth. All pups were infected with MCMV on postnatal day (PND) 0. After 14 days, pups were sacrificed and blood, salivary glands, lungs, spleens and livers collected for examination of viral loads and immune phenotyping.

3.2.2. Single cell suspension from murine organs

Blood, thymi, spleens and bone marrow of the progeny were harvested on PND 1, 3, 5, 10 or PND 28 (week 4). Blood was collected into EDTA tubes. Single cell suspension was performed under sterile conditions by mincing the organs through a cell strainer (70 µm). Erythrocytes in the blood samples were lysated using eBioscience™ 10x RBC Lysis Buffer.

Cells (thymus, spleen, bone marrow, blood) were counted automatically in the NucleoCounter® in a 1:100 dilution using Cell Counting Medium (full RPMI medium). Cells were either directly stained for flow cytometry or frozen and stored at -80 °C for later analysis. For analysis preparation, frozen cells were thawed and taken up in warm RMPI medium.

3.2.3. Cell stimulation

Cells were stimulated using Phorbol-12-myristat-13-acetat (100 µg/ml) and Ionomycin (1 mg/ml) (Sigma-Aldrich, St. Louis, MO, USA) and incubated for 3 h at 37 °C. 30 minutes after stimulation, 0,7 µl Brefeldin (3mg/ml) was added to each tube. For intracellular staining, cells were kept in in X vivo medium (Lonza, Basel, Switzerland) and fixated-permeabilized using the eBioscience™ Anti-human FoxP3 Staining Set APC from Invitrogen (Carlsbad, CA, USA) according to the manufacturers' protocol.

3.2.4. Cell staining and flow cytometry

Processed cells were stained for flow cytometry in four panels using following anti-mouse antibodies (Table 2): anti-B220 BV480 (RA3-6B2), anti-CD4 R718 (RM4-5), anti-CD49d BV786 (R1-2), anti-CD127 PE-CF594 (SB/199), Annexin V FITC, anti-CCR6 AF647 (11A9) and anti-Ly6G PerCPCy5.5 (1A8) from BD Biosciences (San Jose, CA, USA); anti-CD44 FITC (IM7), anti-CD45 PE-Cy7 (30-F11), anti-IFNγ PE (XMG1.2), anti-KLRG1 APC-Cy7 (2F1/KLRG1), anti-TCRβ BV605 (H57-597), anti-TCRβ PerCPCy5.5 (H57-597), anti-TCRγδ BV605 (GL3), anti-B220 BV785 (RA3-6B2), anti-CD117 PerCPCy5.5 (2B8), anti-CD11b FITC (M1/70), anti-CD11b Pe-Cy7 (M1/70), anti-CD11c BV421 (N418), anti-CD127 BV421 (A7R34), anti-CD135 BV421 (A2F10), anti-CD25 BV650 (PC61), anti-CD25 BV421 (PC61), anti-CD27 PE (I.G.3A10), anti-CD3 PE (145-2C11), anti-CD3 PECy7 (145-2C11), anti-CD4 PerCP (RM4-5), anti-CD4 AF700 (RM4-5), anti-CD44 APC-Cy7 (IM7), anti-CD45 AF700 (30-F11), anti-CD45 APC-Cy7 (30-F11), anti-CD48 AF-700 (HM48-1), anti-CD69 BV785 (H1.2F3), anti-CD8a APC-Cy7 (53-6.7), anti-CD8a BV650 (53-6.7), anti-Gr-1 Pe-Cy7 (RB6-865), anti-IgM PE (RMM-1), anti-Ly6D FITC (49-H4), anti-MHCII BV785 (M5/114.15.2), anti-NK1.1 PE-Cy7 (PK136) and anti-Sca-1 APC (D7) from BioLegend (San Diego, CA, USA); anti-TCRγδ APC (eBioGL3), anti-CD19 PE-

Cy7 (1D3) from eBioscience (San Diego, CA, USA). Data was acquired on a 12-Color FACS Celesta (BD Biosciences San Jose, CA, USA) and on the FACSymphony A1 Cell Analyzer (BD Biosciences San Jose, CA, USA) and manually gated and analyzed using FlowJo ® Software (Tree Star, Ashland, OR, USA).

Table 2: Summary of flow cytometry panels.

FACS Celesta				FACS Symphony A1	
Panel	1	2	3	4	
BV421/V450	CD135	CD25	CD11c | CD127	BV421	CD25
BV510/V500/Pacific Orange	Viability	Viability	Viability	BV480	Viability | B220
BV605	---	TCRβ	TCRγδ	BV605	TCRγδ
BV650	---	CD8a	CD25	BV786	CD8
BV785	B220	CD69	MHCII	FITC	CD49d
FITC	Ly6D	Annexin V	CD11b	PerCP-Cy5.5	CD44
PE	IgM	CD27	---	PE	TCRβ
PerCP/PerCPCy5.5	CD117	CD117	Ly6G | CD4	PE-CF594	IFN-γ
PE-Cy7	CD3 | CD11b | Gr-1	CD3	CD19 | NK1.1	PE-Cy7	CD45
APC/eFluor450/AF647	Sca-1	TCRγδ	CCR6	AF647	CD122
AF700	CD48	CD4	CD45	R718	CD4
APC-Cy7/AF750/APC-eFluor780	CD45	CD44	CD8	APC-H7	KLRG1

3.2.5. Gating strategy

Leukocytes (panel 1-4) were gated according to granularity and size (FSC-A versus SSC-A), followed by removal of doublets with a FSC-A versus FSC-H diagonal gate and a second removal of doublets with a SSC-A versus SSC-H diagonal gate. Representative hierarchical gating strategies for panels 1-4 are depicted in Supplementary Figures S1-S4 in the appendix.

3.2.6. Luciferase assay

Harvested lungs, salivary glands, livers and spleens were kept on ice-cooled PBS, homogenized with TissueLyser II (Qiagen) at 25 Hz for 2 minutes and centrifuged at 20.000 g for 15 minutes. Supernatants were measured for luciferase expression by quantification of luminescence after the addition of native coelenterazine (Synchem) with Centro XS³ LB

960 (Berthold Technologies). Infections and infection readouts were performed in the laboratory AG Stahl by F. Stahl, S. Tödter and L. Fonseca Brito.

3.2.7. Study approval

All animal experiments were performed in accordance with national and institutional guidelines on animal care and ethics were approved by the local animal ethics committee (Behörde für Gesundheit und Verbraucherschutz, Amt für Verbraucherschutz, Freie und Hansestadt Hamburg, reference number: N19/094).

3.2.8. Statistics

Statistics were performed with GraphPad Prism software (La Jolla, CA, USA). Outliers were identified using the ROUT method, p-values were calculated using the non-parametric Mann-Whitney Test. Significance is indicated as follows: * $p < 0.05$, ** $p < 0.01$, ***$p < 0.001$, and **** $p < 0.0001$.

4. Results

4.1. Transient reduction of hematopoietic progenitor cells in murine bone marrow after prenatal betamethasone treatment

The impact of prenatal betamethasone on immune cell development, starting from HSCs in the bone marrow, continuing with their differentiation in the thymus and their seeding to the bloodstream and spleen was investigated using our established pregnancy murine model depicted in Figure 5 (Diepenbruck *et al.*, 2013; Gieras *et al.*, 2017). Animal weights were slightly higher in betamethasone-exposed animals on PND 3 and 10, but normalized after 4 weeks (Figure 7).

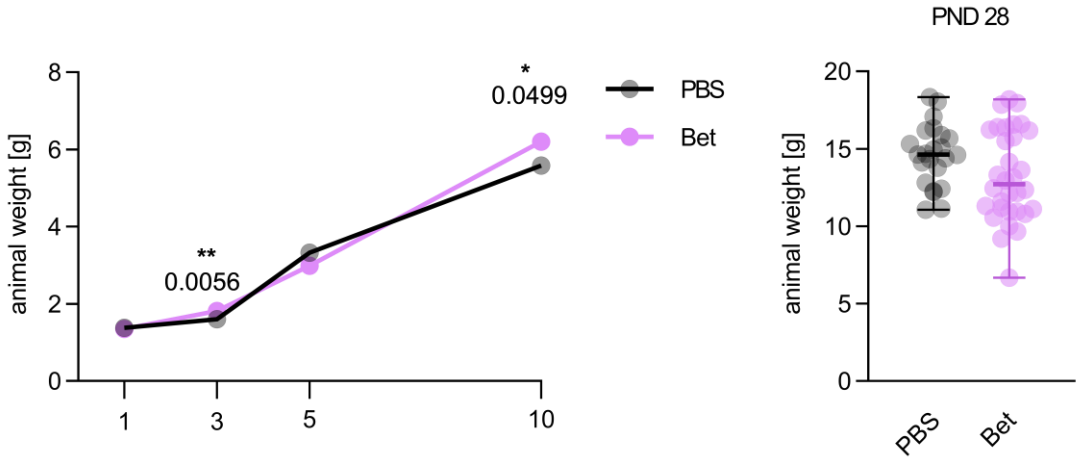

Figure 7: Weight differences between prenatally betamethasone treated animals and controls. Body weight from prenatally betamethasone treated (Bet) and untreated (PBS) animals on postnatal days (PND) 1, 3, 5 and 10. Pink circles and pink lines represent medians after antenatal betamethasone exposure (Bet). Black squares and black lines represent medians of PBS treated vehicle controls (PBS). n = 7-13 mice per group and time point, both female and male animals. Lines represent medians. Outliers were excluded with ROUT method. Non-parametric Mann-Whitney test was used for statistical analysis, * $p < 0.05$, ** $p < 0.01$.

The absolute cell counts in the bone marrow were very similar in betamethasone-exposed and control animals (Figure 8). In order to gain further insight into early leukopoiesis, a detailed phenotypic analysis of bone marrow cells was performed. A flow cytometry antibody panel was established that allows to discriminate different subsets of hematopoietic precursor cells, including early progenitors (Lin^-, $Sca1^+$, $cKit^+$ LSK cells), common myeloid progenitors (CMPs; Lin^-, $Sca1^-$, $cKit^+$, $CD48^+$), common lymphoid

progenitors (CLPs; Lin^-, $cKit^-$, $Ly6D^-$, $CD135^+$) and B cell-committed lymphoid progenitor cell (BLP; Lin^-, $cKit^-$, $Ly6D^+$, $CD135^-$) (Panel 1, Supplementary Figure S1).

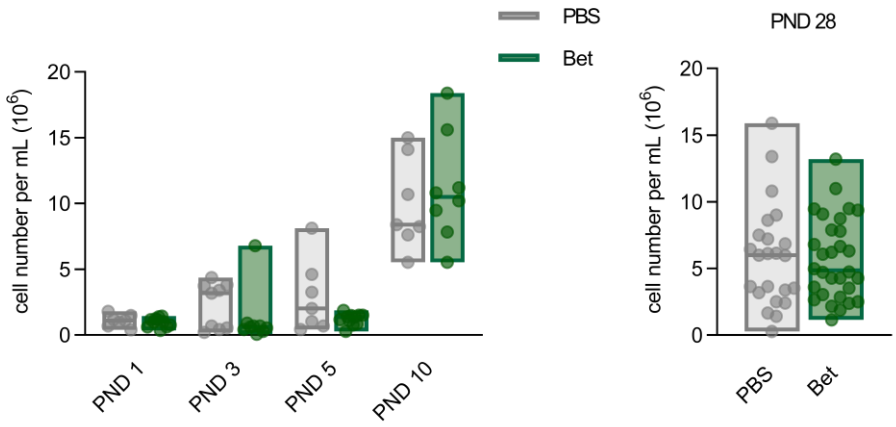

Figure 8: Overall cell counts in bone marrow after ACS treatment. Cell numbers in prenatally betamethasone-treated and PBS vehicle control treated animals on PND 1, 3, 5, 10 and 28 were assessed by automatic cell counting. Green circles and boxes represent mice after antenatal betamethasone exposure (Bet). Grey circles and boxes represent PBS treated vehicle controls (PBS). Horizontal lines represent medians. n = 7-31 mice per group and time point, both female and male animals. Lines represent medians. Outliers were excluded with ROUT method. Non-parametric Mann-Whitney test was used for statistical analysis, * $p < 0.05$, ** $p < 0.01$.

The number of earliest, multipotent progenitors (LSK cells) were similar in the first 10 PNDs in betamethasone-exposed and control animals, however, LSK cell counts were generally very low during the first PNDs, making it difficult to compare between treatments. On day 28, LSK counts were higher in betamethasone-exposed animals (Figure 9a). After the initial step of leukocyte development, LSKs differentiate into either CMPs or CLPs (Rieger and Schroeder, 2012). Both CMP and CLP counts were slightly lower but not substantially altered after ACS treatment in comparison to the control (Figure 9b and c).

After committing to the lymphoid lineage, CLPs give rise to either pro-T cells that further develop in the thymus or BLPs (Inlay *et al.*, 2009; Rieger and Schroeder, 2012). In our model, prenatal betamethasone exposure led to a slightly lower number of BLPs on PND 10 and increased number of BLPs on day 28 (mean of 54227 cells Bet vs. 37272 cells PBS control, respectively, p=0.0728) (Figure 9d), hinting towards enhanced hematopoiesis between postnatal week 2 and 4 in ACS-exposed pups.

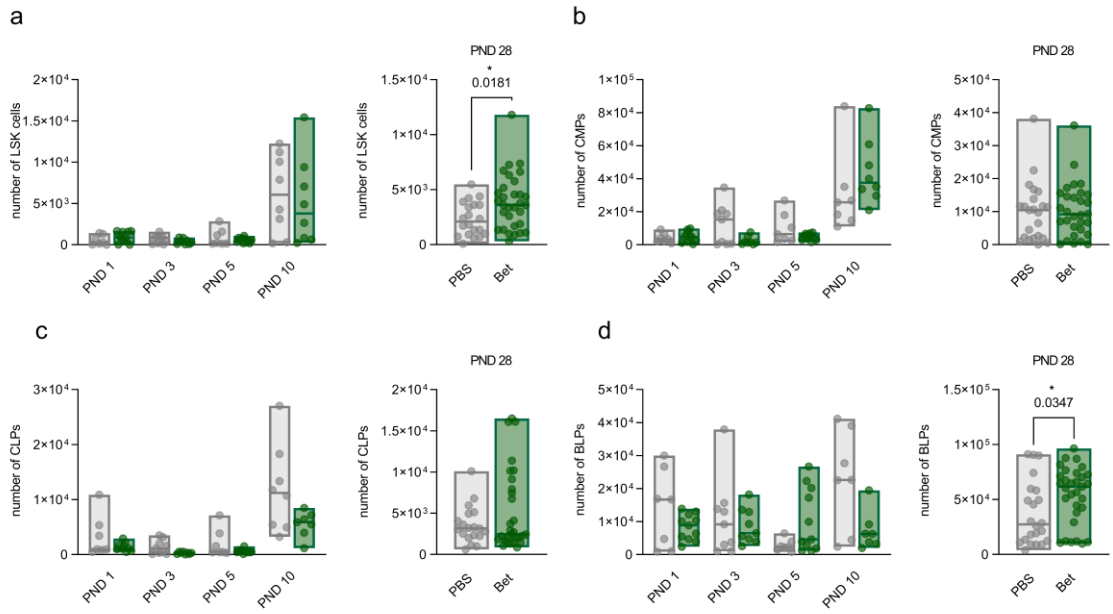

Figure 9: Effects of ACS treatment on leukopoiesis in murine bone marrow. (a) Absolute numbers of $Lin^{-}Sca1^{+}cKit^{+}$ (LSK) cells, (b) common myeloid progenitors (CMPs), (c) common lymphoid progenitors (CLPs), (d) B-cell committed lymphoid progenitors (BLPs) and of either ACS exposed (Bet) or control (PBS) animals were assessed by flow cytometry on postnatal day 1, 3, 5, 10 and 28. Green circles and boxes represent mice after antenatal betamethasone exposure (Bet). Grey circles and boxes represent PBS treated vehicle controls (PBS). Horizontal lines represent medians. n = 7-31 mice per group and time point, both female and male animals. Lines represent medians. Outliers were excluded with ROUT method. Non-parametric Mann-Whitney test was used for statistical analysis, * $p < 0.05$, ** $p < 0.01$.

B cell precursors undergo several maturation steps before differentiating into immature B cells that are fully functional, but have yet to leave bone marrow and migrate to peripheral immunological tissues. The definite B cell precursors are pro- and pre-B cells (Hardy and Hayakawa, 2001), which both were not significantly affected by ACS administration (data not shown). Immature B cell counts were significantly reduced on PND 3 in betamethasone-exposed animals and remained lower than in controls until day 10 (Figure 10).

Taken together, these results suggest that ACS treatment negatively affects early hematopoiesis and lymphopoiesis. Interestingly, LSKs and BLPs were increased after four weeks, suggesting a compensatory overproduction of lymphoid progenitors in ACS-treated pups in order to refill the niche.

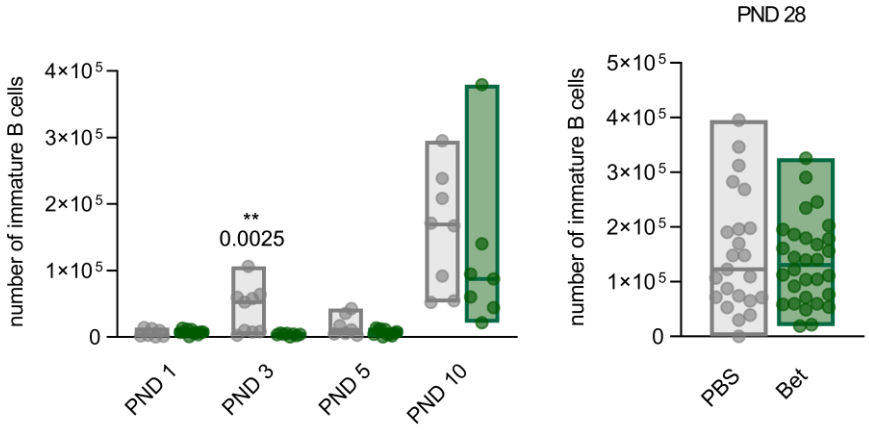

Figure 10: Immature B cells in bone marrow after ACS treatment. Immature, IgM⁺ B cells of either ACS exposed (Bet) or control (PBS) animals were assessed by flow cytometry on postnatal day 1, 3, 5, 10 and 28. Green circles and boxes represent mice after antenatal betamethasone exposure (Bet). Grey circles and boxes represent PBS treated vehicle controls (PBS). Horizontal lines represent medians. n = 7-31 mice per group and time point, both female and male animals. Lines represent medians. Outliers were excluded with ROUT method. Non-parametric Mann-Whitney test was used for statistical analysis, * $p < 0.05$, ** $p < 0.01$.

4.2. Depletion of thymocytes in all developmental stages after prenatal betamethasone exposure

Prenatal betamethasone administration has been shown to cause a reduction of the thymic volume in the perinatal period in humans and mice and alter T cell development at birth in a murine model of ACS (Diepenbruck *et al.*, 2013; Gieras *et al.*, 2017). In order to investigate the effects of prenatal GCs on seeding of T cells into the periphery, an analysis of developing murine thymocytes in the first four weeks of life was performed via flow-cytometry (Panel 2, Supplementary Figure S2). Although there were no substantial differences in thymic weight ratios between both groups in the first four postnatal weeks (Figure 11), thymocyte counts were significantly lower in betamethasone-exposed animals on PNDs 1 and 5, normalized by day 10, and maintained at 4 weeks (Figure 12).

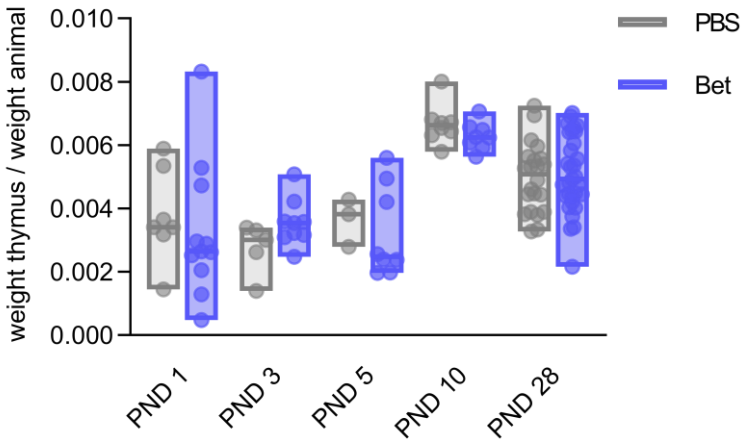

Figure 11. Thymus weight ratios after prenatal betamethasone exposure. Thymus weight ratios of ACS exposed (Bet) or PBS control (PBS) animals on PND 1, 3, 5, 10 or 28. Ratios represent the quotient of organ weight in grams and animal weight in grams. Blue circles and boxes represent mice after antenatal betamethasone exposure (Bet). Grey circles and boxes represent PBS treated vehicle controls (PBS). Horizontal lines represent medians. n = 7-32 mice per group and time point, both female and male animals. Lines represent medians. Outliers were excluded with ROUT method. Non-parametric Mann-Whitney test was used for statistical analysis, * $p < 0.05$, ** $p < 0.01$.

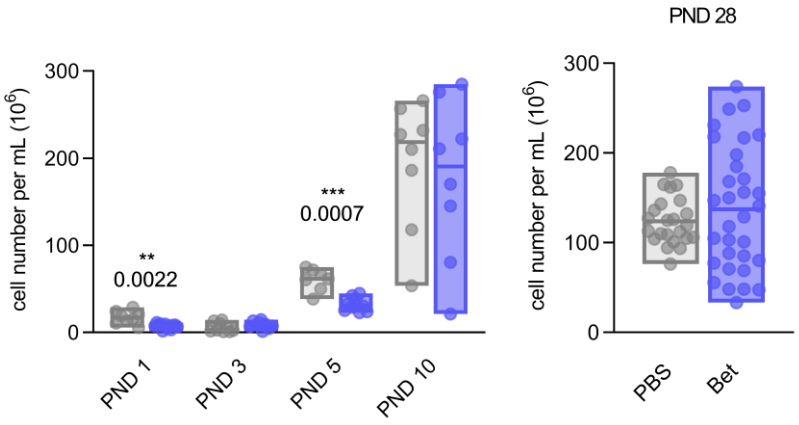

Figure 12: Overall cell counts in thymus after ACS treatment. Cell counts in prenatally betamethasone-treated and PBS vehicle control treated animals on PND 1, 3, 5, 10 and 28 were assessed by automatic cell counting. Blue circles and boxes represent mice after antenatal betamethasone exposure (Bet). Grey circles and boxes represent PBS treated vehicle controls (PBS). Horizontal lines represent medians. n = 7-32 mice per group and time point, both female and male animals. Lines represent medians. Outliers were excluded with ROUT method. Non-parametric Mann-Whitney test was used for statistical analysis, * $p < 0.05$, ** $p < 0.01$.

A reduction in thymocytes on postnatal day 1 and 5 was seen throughout all developmental stages of thymocytes, starting with double negative (DN) thymocytes, where all DN subpopulations DN1-DN4 were equally affected (Figure 13 a-e).

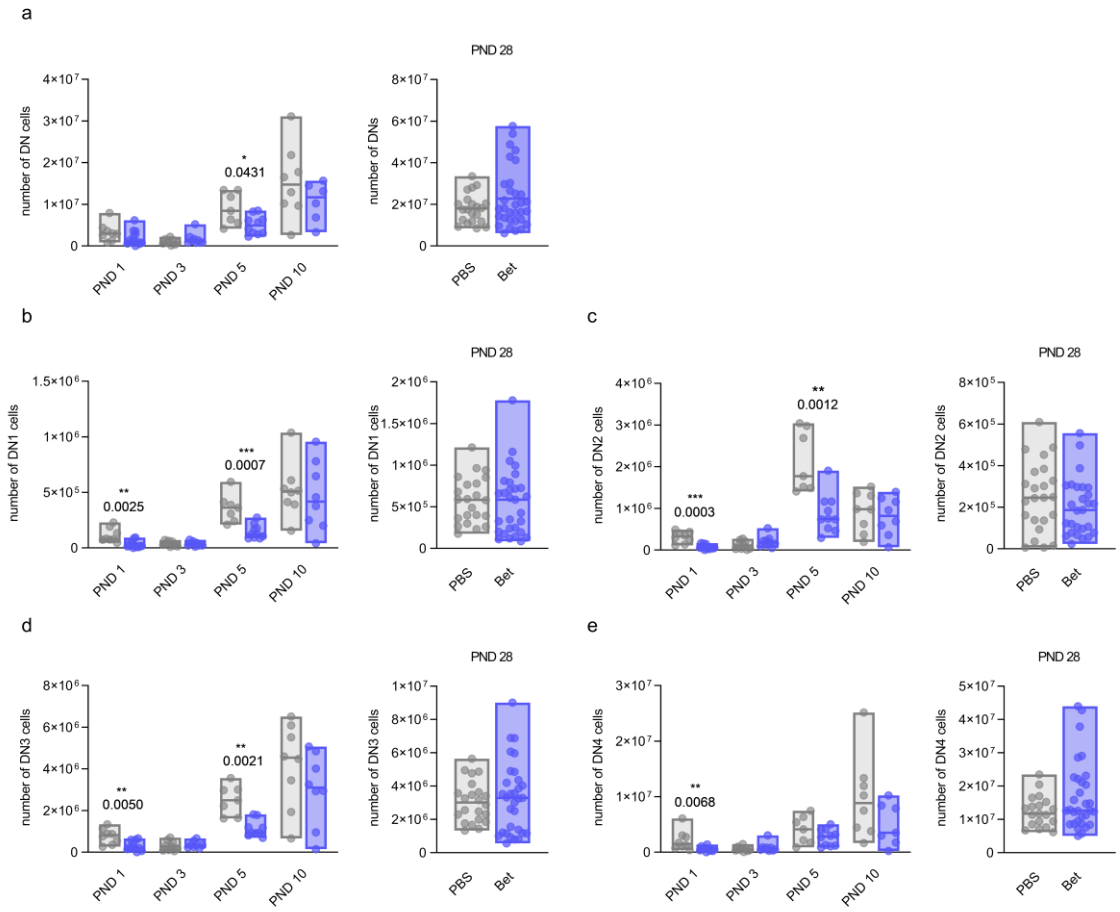

Figure 13: Alterations in DN thymocytes after prenatal ACS treatment. Absolute numbers of (a) overall CD4- CD8- Double negative (DN) cells, (b) $CD44^+$ $CD25^-$ DN1 cells, (c) $CD44^+$ $CD25^+$ DN2 cells, (d) $CD44^-$ $CD25^+$ DN3 cells and (e) $CD44^-$ $CD25^-$ DN4 cells of ACS exposed (Bet) or control (PBS) animals were assessed by flow cytometry on postnatal day 1, 3, 5, 10 and 28. Blue circles and boxes represent mice after antenatal betamethasone exposure (Bet). Grey circles and boxes represent PBS treated vehicle controls (PBS). Horizontal lines represent medians. n = 7-32 mice per group and time point, both female and male animals. Lines represent medians. Outliers were excluded with ROUT method. Non-parametric Mann-Whitney test was used for statistical analysis, * $p < 0.05$, ** $p < 0.01$.

Immature CD8 single positive thymocytes (ISP8), pre-selection double positive (DP) and post-selection ($TCR\beta^+$) DP thymocytes, and finally, both CD4 and CD8 single positive thymocytes (CD4 SP, CD8 SP) showed lower cell numbers after ACS exposure on PND 1 and 5 and recovered by postnatal day 10 (Figure 14 a-e). This data confirms the depletion of all main thymocyte populations shortly after prenatal betamethasone treatment, and recovery between PNDs 5 and 10.

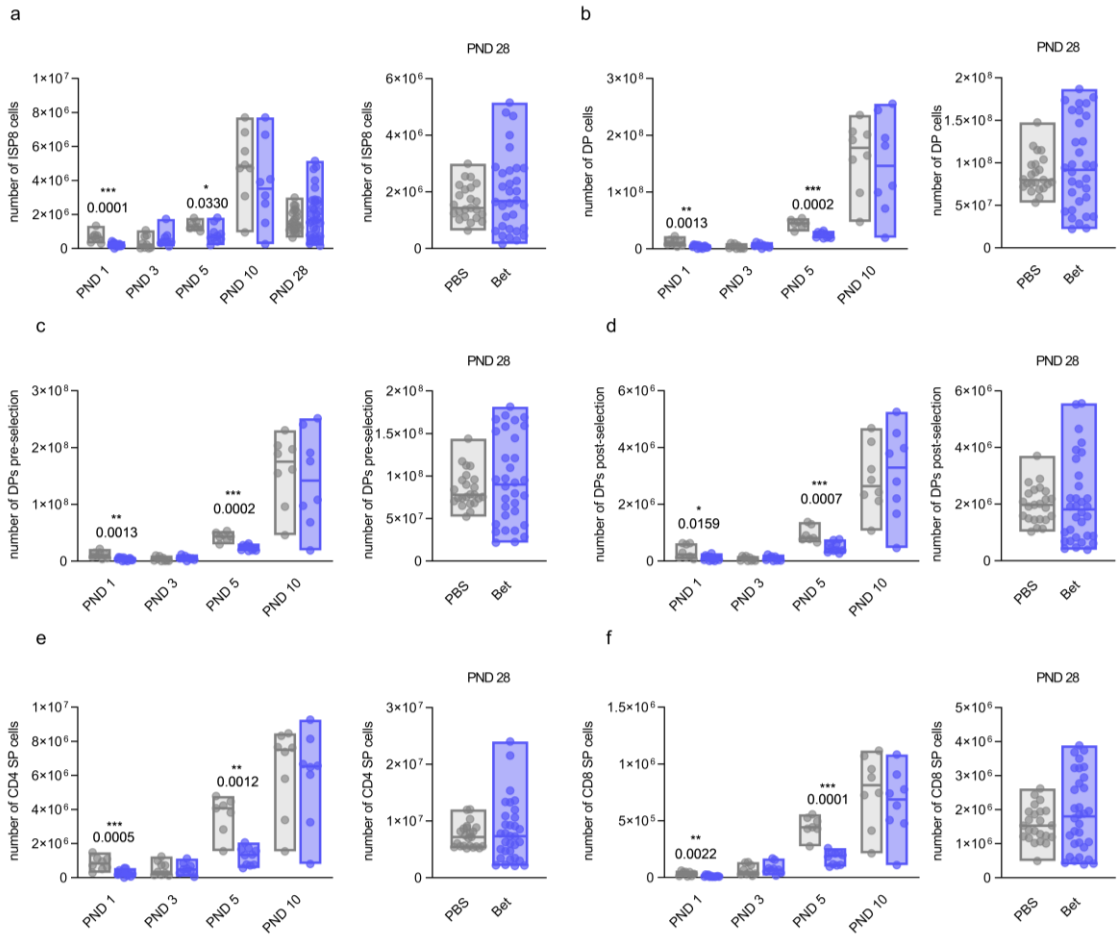

Figure 14: Alterations in thymocyte counts after prenatal betamethasone treatment. Absolute numbers of (a) ISP8, (b) overall DP thymocytes, (c) pre-selection DPs, (d) post-selection DPs, (e) CD4 single positive and (f) CD8 single positive T cells in prenatally betamethasone-treated and PBS vehicle control treated animals were assessed by flow cytometry on postnatal day 1, 3, 5, 10 and 28. Blue circles and boxes represent mice after antenatal betamethasone exposure (Bet). Grey circles and boxes represent PBS treated vehicle controls (PBS). n = 7-32 mice per group and time point, both female and male animals. Lines represent medians. Outliers were excluded with ROUT method. Non-parametric Mann-Whitney test was used for statistical analysis, * $p < 0.05$, ** $p < 0.01$.

Besides the main thymocyte populations, unconventional T cell types in the thymus were investigated. Regulatory T cells are known to be more resistant to steroid exposure compared to other thymocyte populations (Chen *et al.*, 2004; Gieras *et al.*, 2017; Ugor *et al.*, 2018). Frequencies of regulatory T cells were higher in ACS-treated animals on PND 3, however, the difference disappears already at day 5 (Figure 15). γδT cells behaved in a similar manner as conventional T cells and showed lower numbers on postnatal day 1 and 5 in ACS exposed animals (Figure 16).

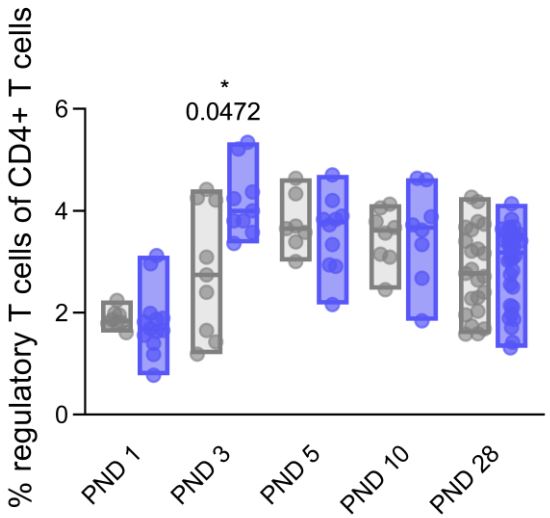

Figure 15: Alterations in frequencies of regulatory T cells in thymus after ACS exposure. Frequency of $CD25^+$ regulatory T cells of $CD4^+$ cells in prenatally betamethasone-treated and PBS vehicle control treated animals were assessed by flow cytometry on postnatal day 1, 3, 5, 10 and 28. Blue circles and boxes represent mice after antenatal betamethasone exposure (Bet). Grey circles and boxes represent PBS treated vehicle controls (PBS). Horizontal lines represent medians. n = 7-32 mice per group and time point, both female and male animals. Lines represent medians. Outliers were excluded with ROUT method. Non-parametric Mann-Whitney test was used for statistical analysis, * $p < 0.05$, ** $p < 0.01$.

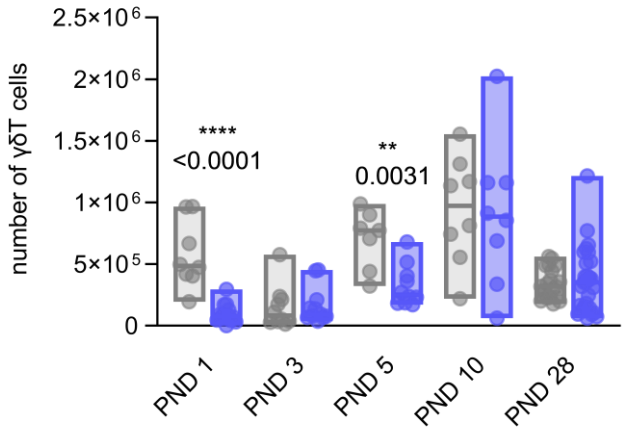

Figure 16: Alterations in γδT cell counts in thymus after ACS exposure. Absolute numbers of γδT cells on PND 1, 3, 5, 10 and 28 in prenatally betamethasone-treated and PBS vehicle control treated animals were assessed by flow cytometry. Blue circles and boxes represent mice after antenatal betamethasone exposure (Bet). Grey circles and boxes represent PBS treated vehicle controls (PBS). Horizontal lines represent medians. n = 7-32 mice per group and time point, both female and male animals. Lines represent medians. Outliers were excluded with ROUT method. Non-parametric Mann-Whitney test was used for statistical analysis, * $p < 0.05$, ** $p < 0.01$.

In summary, these experiments provide evidence that ACS treatment depletes thymocytes in the first week of life. All developmental stages were similarly affected, suggesting an unselective effect of prenatal GCs on developing thymocytes.

4.3. Delayed seeding of immune cells in murine spleen following ACS treatment

Given the influence of ACS treatment on early T and B cell progenitors in the first week of life, the effects of prenatal betamethasone on peripheral immune cell seeding were analyzed next. A flow-cytometry panel was designed in order to gain further insight into splenic lymphoid and myeloid cell compartments (Panel 3, Supplementary Figure S3).

The weight of the spleens in relation to body weight were not significantly affected by prenatal betamethasone (Figure 17).

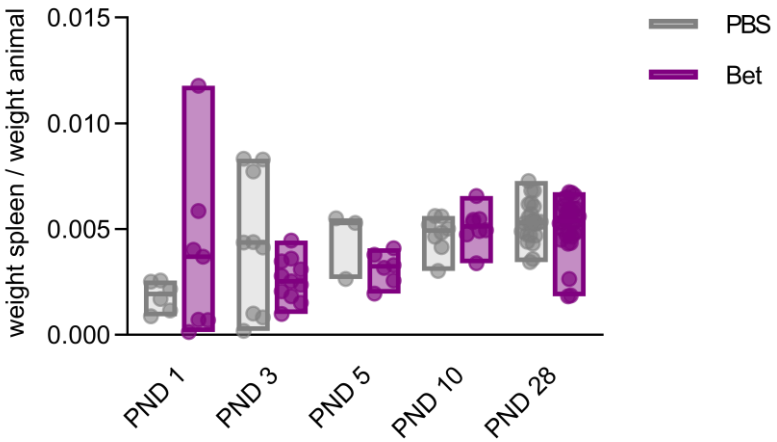

Figure 17: Spleen weight ratios after prenatal betamethasone exposure. Spleen weight ratios of ACS exposed (Bet) or PBS control (PBS) animals on PND 1, 3, 5, 10 or 28. Ratios represent the quotient of organ weight in grams and animal weight in grams. Pink circles and boxes represent mice after antenatal betamethasone exposure (Bet). Grey circles and boxes represent PBS treated vehicle controls (PBS). Horizontal lines represent medians. n = 7-32 mice per group and time point, both female and male animals. Lines represent medians. Outliers were excluded with ROUT method. Non-parametric Mann-Whitney test was used for statistical analysis, * $p < 0.05$, ** $p < 0.01$.

However, absolute cell counts were significantly lower in ACS-exposed pups on PND 5. By PND 10, cell counts where higher in spleens of ACS-exposed pups (Figure 18), suggesting an overcompensation of leukocytes that fill up the niche caused by the previous reduction. After four weeks, cell counts were similar in ACS-exposed animals and controls.

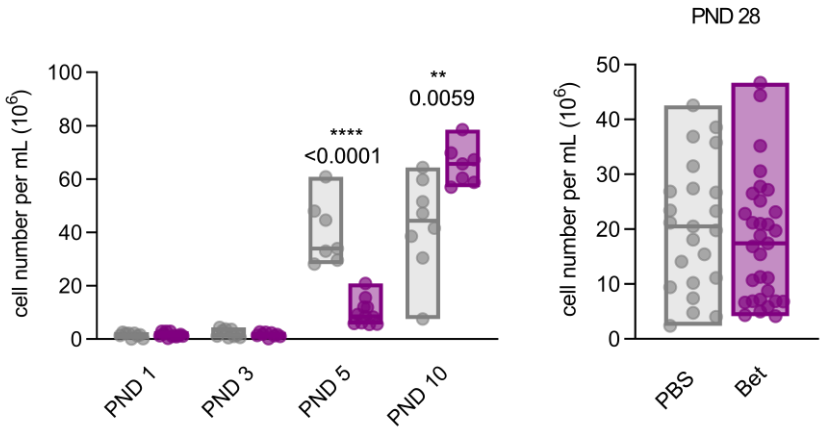

Figure 18: Overall cell counts in spleen after ACS treatment. Cell counts in prenatally betamethasone treated and PBS vehicle control treated animals on PND 1, 3, 5, 10 and 28 were assessed by automatic cell counting. Pink circles and boxes represent mice after antenatal betamethasone exposure (Bet). Grey circles and boxes represent PBS treated vehicle controls (PBS). Horizontal lines represent medians. n = 7-32 mice per group and time point, both female and male animals. Lines represent medians. Outliers were excluded with ROUT method. Non-parametric Mann-Whitney test was used for statistical analysis, * $p < 0.05$, ** $p < 0.01$.

The effect of ACS treatment was consistent across T cells, B cells, NK cells and granulocytes and showed lower cell numbers after prenatal betamethasone on PND 5 and (over-) compensations on PND 10 (Figure 19).

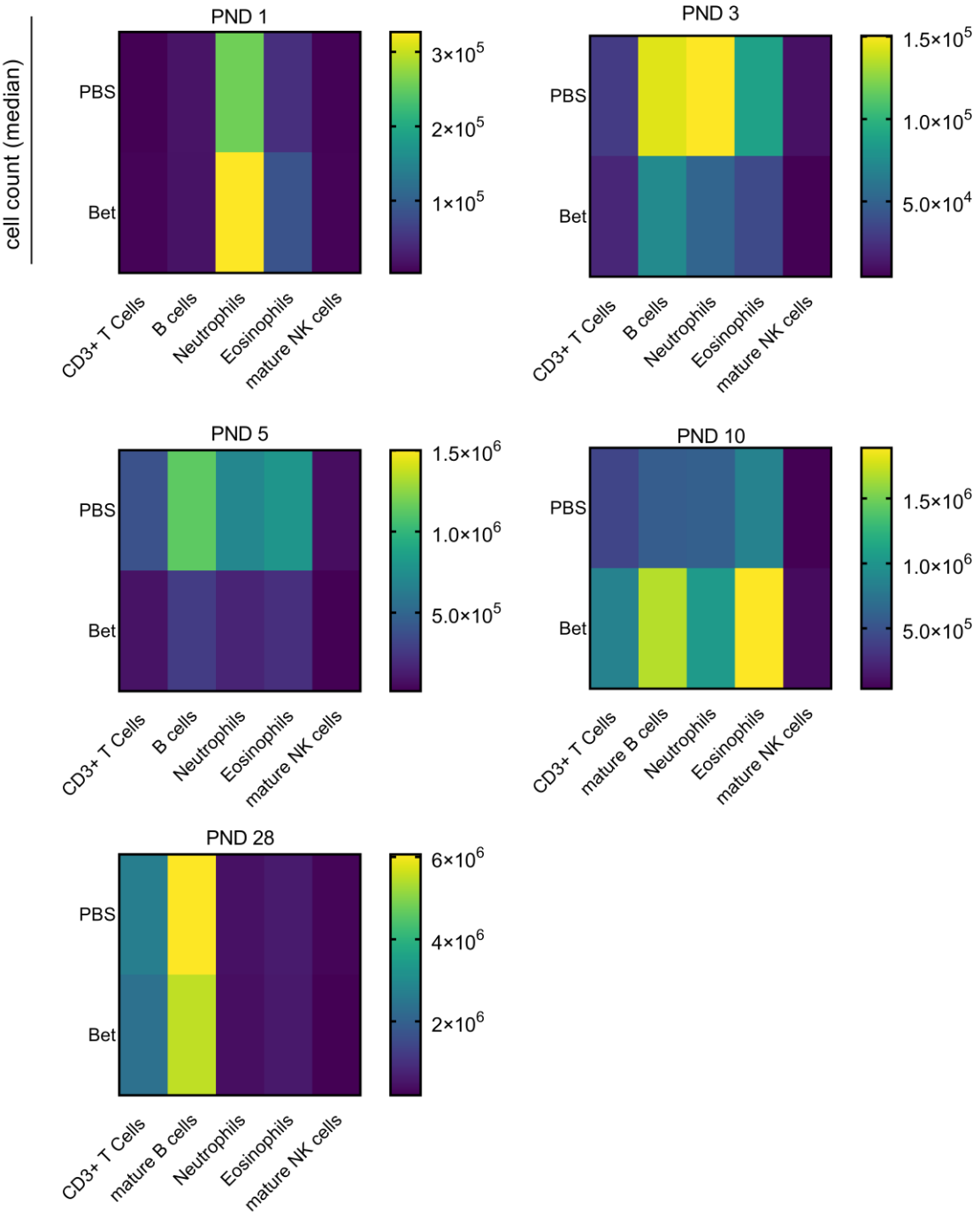

Figure 19: Adaptive and innate immune cell populations in spleen after ACS exposure. Heatmap representation of median cell counts of T cells, B cells, Neutrophils, Eosinophils and NK cells in prenatally betamethasone-treated and PBS vehicle control treated animals were assessed by flow cytometry on PND 1, 3, 5, 10 and 28. n = 7-32 mice per group and time point, both female and male animals. Outliers were excluded with ROUT method. Non-parametric Mann-Whitney test was used for statistical analysis, * $p < 0.05$, ** $p < 0.01$.

Next, it was investigated whether particular subpopulations of splenic T cells were specifically affected by ACS treatment. ACS treatment led to a shift in composition of the $CD3^+$ compartment. The frequency of T cells ($CD3^+$) (Figure 20a) decreased proportionally to total cell counts, reflecting the general depletion of leukocytes following prenatal betamethasone administration.

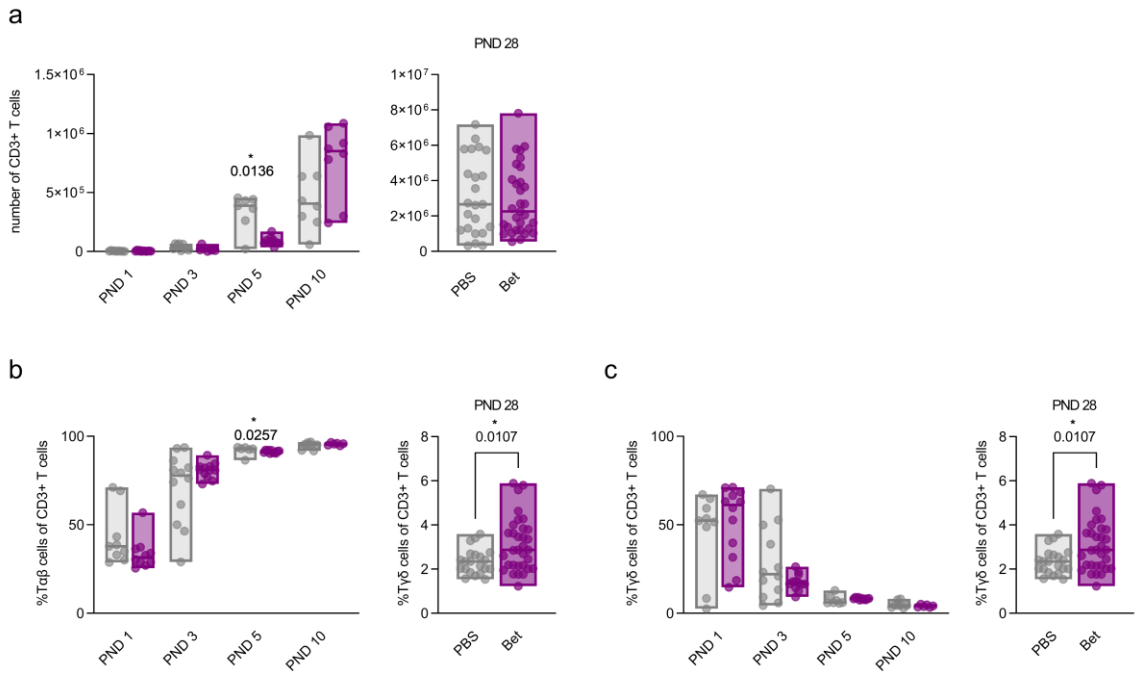

Figure 20: Alterations in the T cell compartment of neonatal spleens after ACS exposure. (a) Cell counts of $CD3^+$ T cells, (b) frequency of αβ-T cells and (c) γδ-T cells in prenatally betamethasone-treated and PBS vehicle control treated animals were assessed by flow cytometry on PND 1, 3, 5, 10 and 28. n = 7-32 mice per group and time point, both female and male animals. Pink circles and boxes represent mice after antenatal betamethasone exposure (Bet). Grey circles and boxes represent PBS treated vehicle controls (PBS). Horizontal lines represent medians Outliers were excluded with ROUT method. Non-parametric Mann-Whitney test was used for statistical analysis, * $p < 0.05$, ** $p < 0.01$.

Frequencies of αβ T cells in spleen were significantly lower on PND 5 and, interestingly, again on day 28 (Figure 20b). In contrast to what was observed in αβ T cells, the frequencies of γδ T cells in the spleen were similar between the ACS and control group until PND 10, but frequencies of γδ T cells were notably higher in spleens of betamethasone-exposed animals at PND 28 (Figure 20c). This data suggests a higher susceptibility of αβ T cells to ACS treatment compared to γδ T cells in secondary lymphoid organs. Elevated γδ T cell frequencies in spleen might be a sign of unconventional T cells compensating for the lack of αβ T cells following ACS treatment.

Conventional CD8⁺ T cells (Figure 21a) and CD4⁺ T cells (Figure 21b) were reduced in parallel to overall CD3⁺ and total cell counts. Although CD4⁺ T cells were generally reduced in both number and frequency, the frequency of CD4⁺ regulatory T cells remained at equal levels after ACS treatment, suggesting a higher resistance to steroids (Figure 21c).

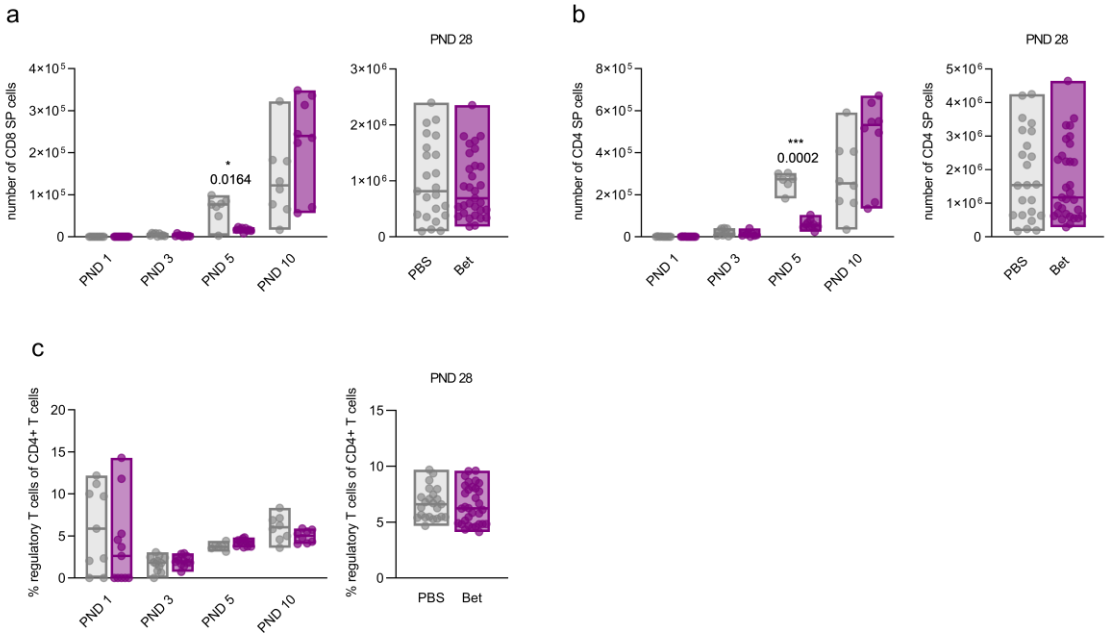

Figure 21: Alterations in counts and frequencies of T cell subtypes in spleen after ACS exposure. Absolute cell counts of (a) CD8⁺ and (b) CD4⁺ thymocytes and frequency of (c) CD25⁺ regulatory T cells of CD4⁺ cells were assessed by flow cytometry on postnatal day 1, 3, 5, 10 and 28. Pink circles and boxes represent mice after antenatal betamethasone exposure (Bet). Grey circles and boxes represent PBS treated vehicle controls (PBS). Horizontal lines represent medians. n = 7-32 mice per group and time point, both female and male animals. Lines represent medians. Outliers were excluded with ROUT method. Non-parametric Mann-Whitney test was used for statistical analysis, * $p < 0.05$, ** $p < 0.01$.

Not only T cells were affected by ACS treatment. B cells in spleens of ACS-exposed animals were also significantly reduced on PND 5. By PND 10, B cell numbers of ACS-exposed animals exceeded those of controls. B cell frequencies did not differ between ACS and control group (Figure 22). Four weeks after birth, cell counts and frequencies were similar in both betamethasone-exposed and control animals.

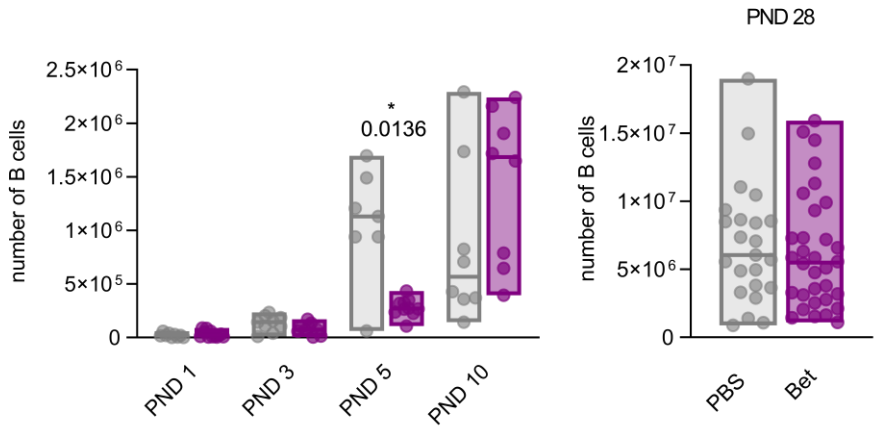

Figure 22: B cells in spleen after ACS treatment. Cell counts of B cells in prenatally betamethasone treated and PBS vehicle control treated animals were assessed by flow cytometry on PND 1, 3, 5, 10 and 28. n = 7-32 mice per group and time point, both female and male animals. Pink circles and boxes represent mice after antenatal betamethasone exposure (Bet). Grey circles and boxes represent PBS treated vehicle controls (PBS). Horizontal lines represent medians Outliers were excluded with ROUT method. Non-parametric Mann-Whitney test was used for statistical analysis, * $p < 0.05$, ** $p < 0.01$.

Next, the impact of ACS treatment on the innate immune system was investigated, focusing on the seeding process in the peripheral compartment. Counts of both neutrophilic (Figure 23a) and eosinophilic (Figure 23c) granulocytes were also significantly reduced in spleens of ACS-exposed animals compared to controls on PNDs 3 and 5 and increased in ACS-treated animals on day 10, while frequencies of neutrophils and eosinophils remained mainly similar between both groups (Figure 23b and d).

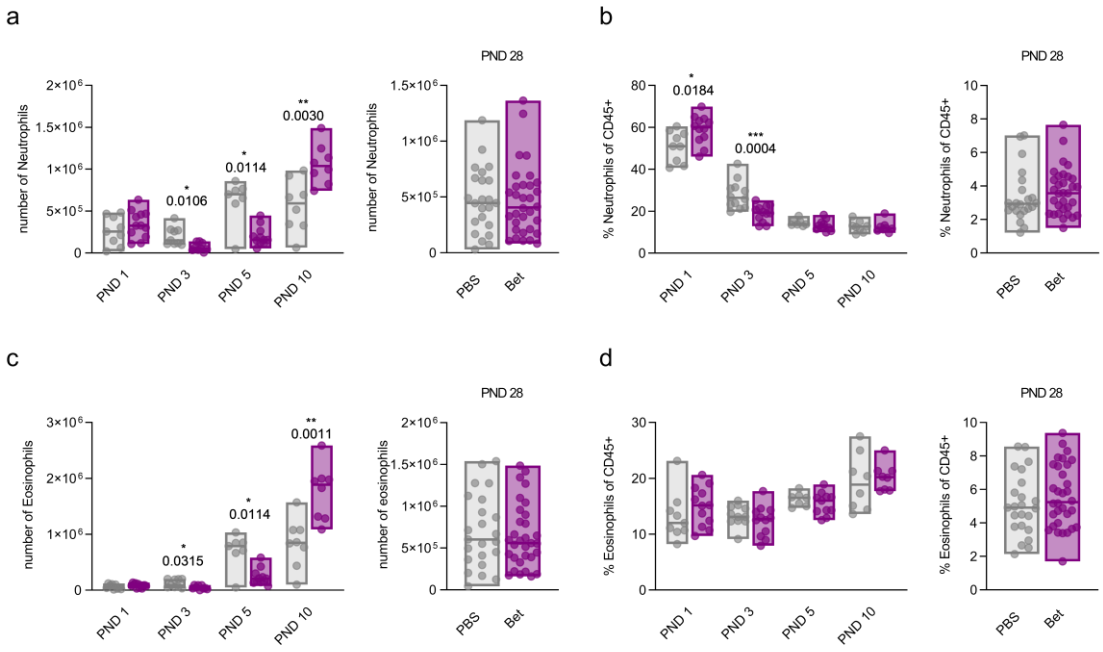

Figure 23: Alterations in granulocyte counts and frequencies in spleen after ACS treatment. (a) Cell counts and (b) frequencies of neutrophils and (c) cell counts and (d) frequencies of eosinophils in prenatally betamethasone-treated and PBS vehicle control treated animals were assessed by flow cytometry on PND 1, 3, 5, 10 and 28. n = 7-32 mice per group and time point, both female and male animals. Pink circles and boxes represent mice after antenatal betamethasone exposure (Bet). Grey circles and boxes represent PBS treated vehicle controls (PBS). Horizontal lines represent medians Outliers were excluded with ROUT method. Non-parametric Mann-Whitney test was used for statistical analysis, * $p < 0.05$, ** $p < 0.01$

It is worth noting that on PND 1, following ACS exposure, the frequencies of neutrophils were increased. This observation is consistent with published data on the phenomenon of neutrophilic demargination that occurs after steroid administration *(Barak, Cohen and Herschkowitz, 1992; Weber* et al.*, 2004)*.

Importantly, in blood there were no significant differences in the frequencies of leukocytes (Figure 24) or between T, B, granulocyte or NK cells (Figure 25) between ACS exposed and control animals.

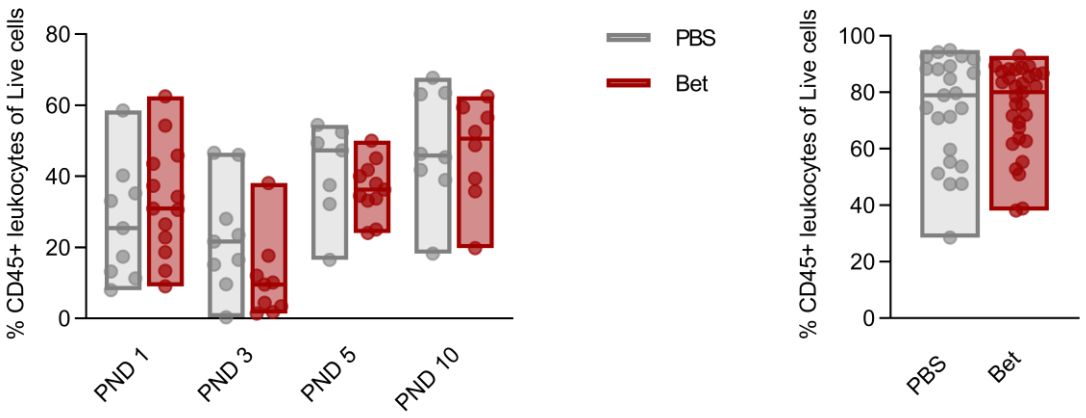

Figure 24: Leukocyte frequencies in blood after ACS treatment. Frequencies of $CD45^+$ cells in blood of prenatally betamethasone-treated and PBS vehicle control treated animals were assessed by flow cytometry on PND 1, 3, 5, 10 and 28. n = 7-32 mice per group and time point, both female and male animals. Red circles and boxes represent mice after antenatal betamethasone exposure (Bet). Grey circles and boxes represent PBS treated vehicle controls (PBS). Horizontal lines represent medians Outliers were excluded with ROUT method. Non-parametric Mann-Whitney test was used for statistical analysis, * $p < 0.05$, ** $p < 0.01$.

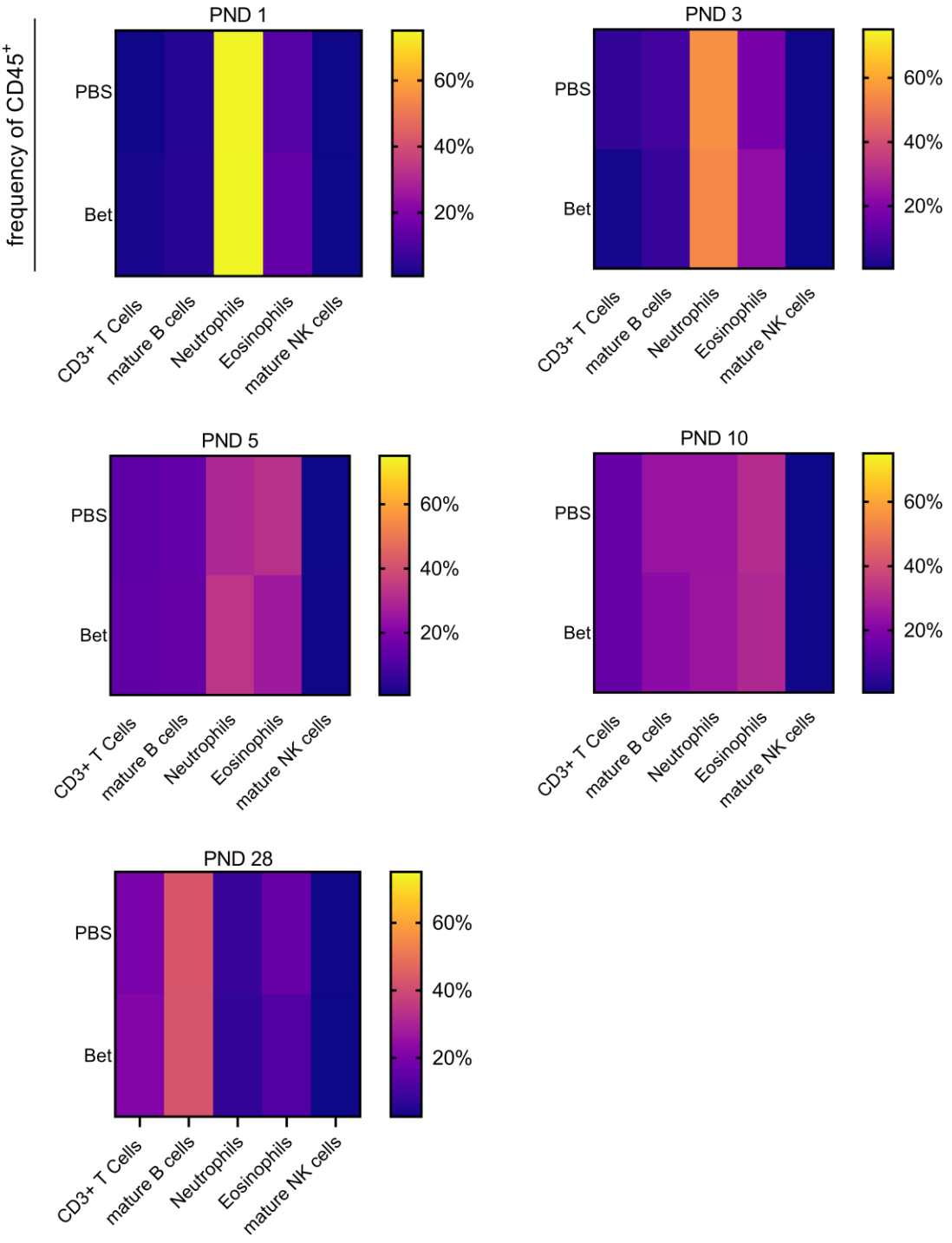

Figure 25: Alterations in leukocyte composition in blood after ACS treatment. Frequencies of T, B, Neutrophils, Eosinophils and mature NK cells in blood of prenatally betamethasone-treated and PBS vehicle control treated animals were assessed by flow cytometry on PND 1, 3, 5, 10 and 28. n = 7-32 mice per group and time point, both female and male animals. Red circles and boxes represent mice after antenatal betamethasone exposure (Bet). Grey circles and boxes represent PBS treated vehicle controls (PBS). Horizontal lines represent medians Outliers were excluded with ROUT method. Non-parametric Mann-Whitney test was used for statistical analysis, * $p < 0.05$, ** $p < 0.01$.

4.4. Immune cell responses to neonatal CMV infection after perinatal steroid treatment

Cytomegalovirus (CMV) infection drives a T cell mediated immune response (Klenerman and Oxenius, 2016; Fonseca Brito, Brune and Stahl, 2019). Since ACS treatment leads to a delayed migration of immune cells, particularly naïve lymphocytes, the consequences of this delay on the clearance of neonatal viral infections were investigated. The use of an established neonatal murine CMV (MCMV) infection model (Figure 6) allowed combining two perinatal challenges, betamethasone exposure and neonatal viral infection (Stahl *et al.*, 2013).

Fourteen days post-infection, viral loads in the lungs of betamethasone-exposed animals were still elevated in comparison to those that received vehicle control, suggesting a reduced clearance of MCMV after betamethasone exposure in this compartment. Viral loads in the remaining tissues (liver, salivary glands, spleen) were not significantly different between betamethasone-exposed and unexposed animals (Figure 26).

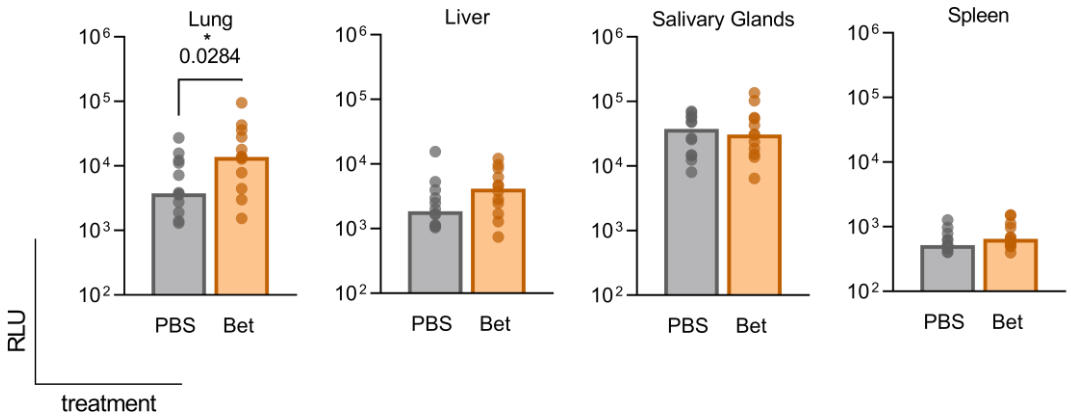

Figure 26: Viral loads following neonatal MCMV infection after neonatal betamethasone. MCMV Viral loads 14 days after infection in lungs, livers, salivary glands and spleens. Samples of neonatally MCMV infected mice and neonatal betamethasone exposure (Bet) or PBS control. Full organs were used on PND 14 for lung, liver, salivary gland measurement, 1/3 spleens were used for spleen analysis. n = 11-15 mice per group, both female and male animals. Boxes represent medians. Outliers were excluded with ROUT method. Non-parametric Mann-Whitney test was used for statistical analysis, * $p < 0.05$, ** $p < 0.01$.

A $CD8^+$ T cell-oriented flow-cytometry panel allowed insights into splenic T cells and IFNγ production after neonatal betamethasone and MCMV exposure (Panel 4, Supplementary Figure S4). Frequencies of splenic $CD4^+$ and $CD8^+$ T cells were similar in betamethasone-treated and untreated animals (Figure 27). In both groups, an inverted CD4/CD8 ratio was

observed (calculated median ratios; 0,63 (PBS); 0,72 (Bet)), indicating increased CD8⁺ T cell levels upon viral activations.

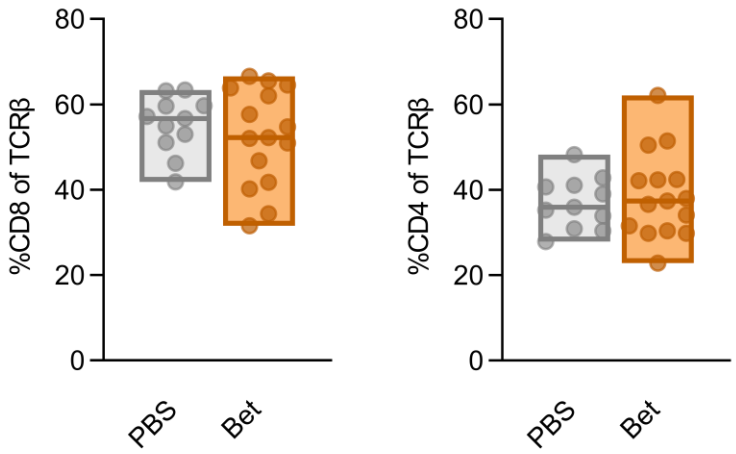

Figure 27: Splenic T cell composition following neonatal MCMV infection and neonatal betamethasone treatment. Frequencies of CD4⁺ and CD8⁺ T cells out of TCRβ⁺ leukocytes on PND 14 after neonatal MCMV infection and either neonatal betamethasone treatment (Bet) or PBS control (PBS). n = 11-15 mice per group, both female and male animals. Lines represent medians. Outliers were excluded with ROUT method. Non-parametric Mann-Whitney test was used for statistical analysis, * $p < 0.05$, ** $p < 0.01$.

The frequencies of IFNγ-production in activated, CD44⁺ CD8SP and CD4SP T cells was comparable between betamethasone treated and control animals (Figure 28).

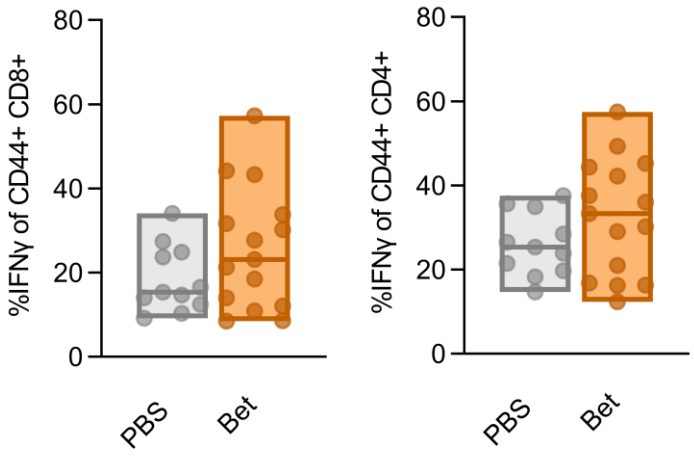

Figure 28: IFNγ expression in spleen after neonatal MCMV infection and neonatal betamethasone. Frequencies of IFNγ+ cells out of CD44⁺ CD8 or CD4 single positive T cells on PND 14 after neonatal MCMV infection and either neonatal betamethasone treatment (Bet) or PBS control (PBS). n = 11-15 mice per group, both female and male animals. Lines represent medians. Outliers were excluded with ROUT method. Non-parametric Mann-Whitney test was used for statistical analysis, * $p < 0.05$, ** $p < 0.01$.

Taken together, in this model viral clearance of MCMV was hampered in the lungs of ACS-exposed animals but cytotoxic T cells showed no significant reduction or difference in IFNγ production after 14 days.

5. Discussion

ACS treatment is crucial for enhancing fetal lung maturation and preventing neonatal respiratory distress syndrome, however, its impact on early hematopoiesis, immune cell migration to the peripheral organs, and the neonatal immune response to infections has not been considered. In this thesis, we found that ACS treatment results in a significant reduction of hematopoietic progenitor cells, developing thymocytes and peripheral lymphoid and innate immune cell populations during the first postnatal days. Cell numbers recovered or even surpassed physiological levels by postnatal day 10. While viral clearance after neonatal MCMV infection was delayed in lungs of steroid exposed animals, perinatal betamethasone showed no effect on IFNγ production in mature cytotoxic T cells.

Immune profiling of cord blood mononuclear cells in a pregnancy cohort (Prenatal Identification of Children's Health, PRINCE) revealed that the frequency of hematopoietic stem and progenitor cells (HSPC) was lower in infants whose mothers that received ACS within the last 14 days before birth (C. Gehbauer and J. Bremer, AG Tolosa, unpublished). However, the reduction of HSPC frequency was not observed when ACS was administered more than 14 days before birth and highlights the regeneration capacity of the hematopoietic niche. These findings align with other studies demonstrating that glucocorticoids impair the proliferation of bone marrow mesenchymal stem cells in a dose-dependent manner and induce autophagy in those cells (Wang *et al.*, 2015). Moreover, apoptosis-related genes are upregulated in HSPCs of patients with Cushing's syndrome, a condition characterized by hyperfunction of the adrenal cortex and chronic exposure to high levels of glucocorticoids (Kawa *et al.*, 2022). In the murine model used for this thesis, ACS treatment led to a transient reduction of immature B cells in the bone marrow, followed by a compensatory rise in lymphoid progenitors four weeks after the treatment. The expression of glucocorticoid receptors makes early B cell progenitors in the human bone marrow highly sensitive to glucocorticoids, with 60-80 % undergoing apoptosis within hours of exposure (Lill-Elghanian *et al.*, 2002). Stress-induced rises in plasma corticosterone

are associated to the mobilization of bone marrow stem and progenitor cells, leading to more circulating mesenchymal stem cells and endothelial progenitor cells (Gao *et al.*, 2021). In this thesis, an increase in LSKs and BLPs in the murine bone marrow was observed four weeks after birth, suggesting that ACS-treated pups may undergo compensatory overproduction of lymphoid progenitors to replenish the niche, potentially driven by GC-induced apoptosis and enhanced mobilization of bone marrow stem and progenitor cells (Igarashi *et al.*, 2001).

ACS-exposed newborns have smaller thymi (Jones et al., 2020; Michie et al., 1998) and previous work from the laboratory AG Tolosa shows that prenatal betamethasone exposure leads to a substantial reduction in thymic volume, induces apoptosis in thymocytes, and alters the T cell receptor repertoire, which may affect development of autoimmunity (Diepenbruck *et al.*, 2013; Gieras *et al.*, 2017; Perna-Barrull *et al.*, 2020). Aligned with these findings, the longitudinal analysis of neonatal murine thymocytes in this thesis demonstrated a marked reduction of thymocytes until PND 5, followed by a progressive regeneration. Remarkably, at 4 weeks of age, the thymus had fully recovered in terms of thymocyte numbers and cellular composition.

Depletion of hematopoietic stem cells and apoptosis of developing thymocytes and early B cells may impact the seeding of secondary lymphoid organs (Landreth, 2002; Shimizu *et al.*, 2023). Indeed, in this study, ACS treatment delayed the seeding of immune cells in the murine spleen. Under physiologic conditions, leukocytes typically populate the neonatal murine spleen by approximately PND 5. However, after ACS treatment, a delay in the seeding by two to three days was observed. This delay was transient, with recovery and even overcompensation of immune cell numbers by day 10, underscoring the plasticity and self-renewal capacity of the neonatal immune system. These findings are consistent with a prior report of reduced splenic T cells following prenatal dexamethasone exposure (Bakker *et al.*, 1995). Glucocorticoids alter leukocyte trafficking through the upregulation of CXCR4 on hematopoietic progenitor cells and on many immune cells including T cells, B cells, monocytes, macrophages, and eosinophils (Nagase *et al.*, 2000; Caulfield *et al.*, 2002; Ghosh *et al.*, 2009; Besedovsky, Born and Lange, 2014; Guo *et al.*, 2017; Cain *et al.*, 2020; Diaz-Jimenez *et al.*, 2020; Perna-Barrull *et al.*, 2023). Increased CXCR4 expression on various immune cell subtypes facilitates chemotaxis, homing, and engraftment which may

explain the elevated cell numbers observed in the spleen at PND 10 following the initial reduction in the ACS mouse model.

Recently, a large national cohort study including more than 2 million births and 45.000 children exposed to ACS reported an increased risk of serious infections, such as sepsis and pneumonia, within the first 12 months of life (Yao *et al.*, 2023). Notably, 40 % of the newborns who received prenatal glucocorticoids were born at term and had an even higher risk of infections than those born preterm (Yao *et al.*, 2023). Investigation of the potential infection-related risks associated with ACS exposure was performed using a CMV infection mouse model that mimics a single course of ACS treatment. An increased viral load in lung tissue was observed, suggesting that ACS treatment hampers viral clearance. In this thesis, T cell function during viral infection was not impaired after a single steroid dose. Continuous perinatal exposure to steroids however alters the HPA axis and impairs antibacterial $CD8^+$ T cell response in mice (Hong *et al.*, 2020). These results underscore the potential impact of repeated dosing, which is sometimes used in clinical practice, as multiple courses of ACS treatment are associated with higher perinatal infection and mortality rates than single dosages (Vermillion, Soper and Newman, 2000; World Health Organization, 2022).

While this thesis provides valuable insights, it is important to acknowledge some limitations, particularly the difference between the immune system of mice and humans (Mestas and Hughes, 2004; Medetgul-Ernar and Davis, 2022). In humans, HSPCs colonize the bone marrow early in embryological development, making it the primary site of hematopoiesis before birth. In contrast, mice exhibit extramedullary hematopoiesis during the first few postnatal days (Dzierzak and Bigas, 2018) and the fetal liver remains the main site of leukopoiesis until birth. Therefore, alterations observed in murine bone marrow are not directly applicable to possible changes in human neonatal immune system development and should be interpreted with caution. In contrast to human pregnancy, the average litter size in mice is around 6 pups per pregnancy (Nagasawa, Miyamoto and Fujimoto, 1973), causing an increased variability in betamethasone exposure among embryos within the same liter, as not all embryos receive the same dose (Diepenbruck *et al.*, 2013). To address this variability, a postnatal steroid/infection model was used to study immune responses under comparable conditions.

ACS treatment saves lives and improves outcomes in preterm infants by promoting lung maturation and reducing mortality and morbidity (Liggins and Howie, 1972; Gyamfi-Bannerman *et al.*, 2016). However, with approximately 40 % of ACS-exposed infants being born at term, careful consideration is needed when deciding to administer this treatment (Ninan *et al.*, 2023).

The work in this thesis demonstrates that ACS induces transient lymphopenia in the bone marrow and thymus, affecting all developmental stages of lymphocytes and delaying the migration of naïve immune cells to peripheral lymphoid organs. Despite this transient disruption, the neonatal immune system shows a remarkable capacity of self-renewal, with recovery occurring within a few days. The potential short- and long-term consequences of this glucocorticoid-induced immune disruption are currently being unveiled in observational cohort studies (Ninan *et al.*, 2023; Räikkönen *et al.*, 2023; Yao *et al.*, 2023). Given that a significant proportion of ACS-treated pregnancies result in term delivery, it is crucial to carefully consider the timing, dosage, and duration of prenatal steroid exposure to minimize adverse effects on the developing immune system.

6. Summary

Antenatal corticosteroids (ACS) are routinely given to women at risk of preterm birth to enhance lung maturation and improve neonatal survival. While the benefits of ACS are well-established, the immune-modulating effects of glucocorticoids, such as thymic atrophy and T cell depletion, raise concerns about potential impacts on neonatal immunity. Although the general effects of glucocorticoids on immune cells are known, the specific consequences of steroid-induced lymphopenia for susceptibility to neonatal infections remain unclear. In this thesis, the effects of prenatal betamethasone exposure on immune cell development and the neonatal response to viral infections were investigated using a pregnancy mouse model. Prenatal steroids reduced lymphoid progenitors and delayed the migration of mature immune cells to the periphery. Despite this, immune responses to neonatal MCMV infection were not significantly compromised by a single dose of steroids, even though viral clearance in the lungs was delayed. In conclusion, antenatal steroid exposure induced a generalized but transient lymphopenia and delayed peripheral seeding of immune cells. However, the neonatal immune system exhibited a strong regenerative capacity, effectively managing the immune response to neonatal MCMV infection even after the challenges posed by a single administration of steroids.

7. Zusammenfassung

Die Antenatale Kortikosteroidtherapie (ANS) wird in der Schwangerschaft im Falle einer drohenden Frühgeburtlichkeit routinemäßig angewandt, um die Lungenreifung des Kindes zu induzieren und somit dessen Überlebenschancen zu verbessern. Die Vorteile pränataler Steroide sind unumstritten, dennoch können erhebliche Veränderungen auf das junge Immunsystem, wie beispielsweise T-Zell-Depletion und Thymusatrophie, festgestellt werden. Das deutet darauf hin, dass es tiefgreifendere Effekte auf das Immunsystem der Nachkommen durch pränatale Steroide geben könnte. Obwohl viel über die allgemeinen immunmodulatorischen Auswirkungen von Glukokortikoiden bekannt ist, gibt es bislang nur wenige Daten zu den spezifischen Folgen von ANS-induzierter Immunzelldepletion im Rahmen von neonatalen Infektionen. In dieser Arbeit wurden die Auswirkungen von pränataler Betamethasongabe auf die Entwicklung von Immunzellen sowie deren Funktion im Rahmen einer neonatalen CMV-Infektion anhand eines Schwangerschaftsmausmodells untersucht. Pränatale Steroide führten zu einer Reduktion von lymphoiden Vorläuferzellen und zu einer verspäteten Migration reifer Immunzellen in die Peripherie. Die Immunantwort auf eine neonatale Infektion mit Cytomegalovirus (MCMV) war jedoch bis auf eine Verzögerung der Viruselimination in der Lunge unbeeinträchtigt.

Zusammenfassend riefen ANS eine generalisierte, aber vorübergehende Lymphopenie in den Neugeborenen hervor und verzögerten die Auswanderung von Immunzellen in die peripheren Organe. Das neonatale Immunsystem bewies jedoch eine starke Regenerationsfähigkeit und konnte auch trotz der steroidbedingten Veränderungen eine CMV-Infektion in der Neugeborenenperiode effektiv bewältigen.

8. References

Abeywickrema, M., Kelly, D. and Kadambari, S. (2023) 'Management of neonatal central nervous system viral infections: Knowledge gaps and research priorities.', *Reviews in medical virology*, 33(2), p. e2421.

Arvin, A. *et al.* (2007) 'Human Herpesviruses: Biology, Therapy, and Immunoprophylaxis', *Human Herpesviruses: Biology, Therapy, and Immunoprophylaxis*. Edited by A. Arvin et al., pp. 10–26.

Bakker, J.M. *et al.* (1995) 'Effects of short-term dexamethasone treatment during pregnancy on the development of the immune system and the hypothalamo-pituitary adrenal axis in the rat', *Journal of Neuroimmunology*, 63(2), pp. 183–191.

Banu, N. *et al.* (1999) 'Modulation of haematopoietic progenitor development by FLT-3 ligand.', *Cytokine*, 11(9), pp. 679–88.

Barak, M., Cohen, A. and Herschkowitz, S. (1992) 'Total leukocyte and neutrophil count changes associated with antenatal betamethasone administration in premature infants', *Acta Paediatrica*, 81(10), pp. 760–763.

Bateman, C.M. *et al.* (2021) 'Cytomegalovirus Infections in Children with Primary and Secondary Immune Deficiencies', *Viruses*, 13(10), p. 2001. A

Benediktsson, R. *et al.* (1997) 'Placental 11 beta-hydroxysteroid dehydrogenase: a key regulator of fetal glucocorticoid exposure.', *Clinical endocrinology*, 46(2), pp. 161–6.

Berek, C., Radbruch, A. and Schroeder, H.W. (2008) 'B-cell development and differentiation', in *Clinical Immunology*. Elsevier, pp. 113–125.

Besedovsky, L., Born, J. and Lange, T. (2014) 'Endogenous glucocorticoid receptor signaling drives rhythmic changes in human T-cell subset numbers and the expression of the chemokine receptor CXCR4', *The FASEB Journal*, 28(1), pp. 67–75.

von Boehmer, H. *et al.* (1998) 'Crucial function of the pre-T-cell receptor (TCR) in TCR beta selection, TCR beta allelic exclusion and alpha beta versus gamma delta lineage commitment.', *Immunological reviews*, 165(1), pp. 111–9.

Boller, S. and Grosschedl, R. (2014) 'The regulatory network of B-cell differentiation: a focused view of early B-cell factor 1 function.', *Immunological reviews*, 261(1), pp. 102–15.

Bonilla, F.A. and Oettgen, H.C. (2010) 'Adaptive immunity', *Journal of Allergy and Clinical Immunology*, 125(2), pp. S33–S40.

Bošnjak, B. *et al.* (2023) 'MCK2-mediated MCMV infection of macrophages and virus dissemination to the salivary gland depends on MHC class I molecules', *Cell Reports*, 42(6), p. 112597.

Bosselut, R. and Vacchio, M.S. (2016) *T-Cell Development*, *T-Cell Development: Methods and Protocols*, pp. 8-9.

de Bruijn, M.F. *et al.* (2000) 'Definitive hematopoietic stem cells first develop within the major arterial regions of the mouse embryo.', *The EMBO journal*, 19(11), pp. 2465–74.

Cain, D.W. *et al.* (2020) 'Murine Glucocorticoid Receptors Orchestrate B Cell Migration Selectively between Bone Marrow and Blood.', *Journal of immunology (Baltimore, Md. : 1950)*, 205(3), pp. 619–629.

Camacho-Gonzalez, A., Spearman, P.W. and Stoll, B.J. (2013) 'Neonatal infectious diseases: evaluation of neonatal sepsis.', *Pediatric clinics of North America*, 60(2), pp. 367–89.

Caulfield, J. *et al.* (2002) 'CXCR4 expression on monocytes is up-regulated by dexamethasone and is modulated by autologous CD3+ T cells', *Immunology*, 105(2), pp. 155–162.

Chabra, S. *et al.* (1998) 'Lymphocyte Subsets in Cord Blood of Preterm Infants: Effect of Antenatal Steroids', *Neonatology*, 74(3), pp. 200–207.

Chang, H.Y. *et al.* (2016) 'Prenatal maternal distress affects atopic dermatitis in offspring mediated by oxidative stress', *Journal of Allergy and Clinical Immunology*, 138(2), pp. 468-475.e5.

Chen, M.J. *et al.* (2011) 'Erythroid/myeloid progenitors and hematopoietic stem cells originate from distinct populations of endothelial cells.', *Cell stem cell*, 9(6), pp. 541–52.

Chen, X. *et al.* (2004) 'Differential response of murine CD4+CD25+ and CD4+CD25- T cells to dexamethasone-induced cell death.', *European journal of immunology*, 34(3), pp. 859–869.

Christensen, J.L. *et al.* (2004) 'Circulation and Chemotaxis of Fetal Hematopoietic Stem Cells', *PLoS Biology*. Edited by Douglas Melton, 2(3), p. e75.

Dagklis, T. *et al.* (2022) 'The use of antenatal corticosteroids for fetal maturation: clinical practice guideline by the WAPM-World Association of Perinatal Medicine and the PMF-Perinatal Medicine foundation', *Journal of Perinatal Medicine*, 50(4), pp. 375–385.

Diaz-Jimenez, D. *et al.* (2020) 'Glucocorticoids mobilize macrophages by transcriptionally up-regulating the exopeptidase DPP4', *The Journal of biological chemistry*, 295(10), pp. 3213–3227.

Diepenbruck, I. *et al.* (2013) 'Effect of prenatal steroid treatment on the developing immune system', *Journal of Molecular Medicine*, 91(11), pp. 1293–1302. A

Ding, L. *et al.* (2012) 'Endothelial and perivascular cells maintain haematopoietic stem cells', *Nature 2012 481:7382*, 481(7382), pp. 457–462.

Dzierzak, E. and Bigas, A. (2018) 'Blood Development: Hematopoietic Stem Cell Dependence and Independence', *Cell Stem Cell*, 22(5), pp. 639–651.

Dzierzak, E. and Speck, N.A. (2008) 'Of lineage and legacy: the development of mammalian hematopoietic stem cells', *Nature Immunology*, 9(2), pp. 129–136.

Fang, F. *et al.* (2011) 'Maternal bereavement and childhood asthma-analyses in two large samples of Swedish children.', *PloS one*, 6(11), p. e27202.

Fonseca Brito, L., Brune, W. and Stahl, F.R. (2019) 'Cytomegalovirus (CMV) Pneumonitis: Cell Tropism, Inflammation, and Immunity', *International Journal of Molecular Sciences*, 20(16), p. 3865.

Gao, W. *et al.* (2021) 'Glucocorticoid guides mobilization of bone marrow stem/progenitor cells via FPR and CXCR4 coupling', *Stem Cell Research & Therapy*, 12(1), p. 16.

Geissmann, F. *et al.* (2010) 'Development of Monocytes, Macrophages, and Dendritic Cells', *Science*, 327(5966), pp. 656–661.

Ghosh, M.C. *et al.* (2009) 'Dexamethasone augments CXCR4-mediated signaling in resting human T cells via the activation of the Src kinase Lck', *Blood*, 113(3), pp. 575–584.

Gieras, A. *et al.* (2017) 'Prenatal administration of betamethasone causes changes in the T cell receptor repertoire influencing development of autoimmunity', *Frontiers in Immunology*, 8, p. 1505.

Gomez Perdiguero, E. *et al.* (2015) 'Tissue-resident macrophages originate from yolk-sac-derived erythro-myeloid progenitors', *Nature*, 518(7540), pp. 547–551.

Grosse, S.D., Ross, D.S. and Dollard, S.C. (2008) 'Congenital cytomegalovirus (CMV) infection as a cause of permanent bilateral hearing loss: a quantitative assessment.', *Journal of clinical virology : the official publication of the Pan American Society for Clinical Virology*, 41(2), pp. 57–62.

Gruver-Yates, A.L., Quinn, M.A. and Cidlowski, J.A. (2013) 'Analysis of glucocorticoid receptors and their apoptotic response to dexamethasone in male murine B cells during development.', *Endocrinology*, 155(2), pp. 463–474.

Guo, B. *et al.* (2017) 'Glucocorticoid hormone-induced chromatin remodeling enhances human hematopoietic stem cell homing and engraftment', *Nature medicine*, 23(4), pp. 424–428.

Gyamfi-Bannerman, C. *et al.* (2016) 'Antenatal Betamethasone for Women at Risk for Late Preterm Delivery', *The New England journal of medicine*, 374(14), pp. 1311–1320.

Hall, T.D. *et al.* (2022) 'Murine fetal bone marrow does not support functional hematopoietic stem and progenitor cells until birth', *Nature Communications*, 13(1), p. 5403.

Hardy, R.R. and Hayakawa, K. (2001) 'B cell development pathways.', *Annual review of immunology*, 19(Volume 19, 2001), pp. 595–621.

Haynes, B.F. and Heinly, C.S. (1995) 'Early human T cell development: analysis of the human thymus at the time of initial entry of hematopoietic stem cells into the fetal thymic microenvironment.', *Journal of Experimental Medicine*, 181(4), pp. 1445–1458.

Hogquist, K.A., Baldwin, T.A. and Jameson, S.C. (2005) 'Central tolerance: learning self-control in the thymus', *Nature reviews. Immunology*, 5(10), pp. 772–782.

Holt, P.G. and Jones, C.A. (2000) 'The development of the immune system during pregnancy and early life', *Allergy*, 55(8), pp. 688–697.

Hong, J.Y. *et al.* (2020) 'Long-Term Programming of CD8 T Cell Immunity by Perinatal Exposure to Glucocorticoids', *Cell*, 180(5), pp. 847-861.e15.

Igarashi, H. *et al.* (2001) 'Age and stage dependency of estrogen receptor expression by lymphocyte precursors', *Proceedings of the National Academy of Sciences of the United States of America*, 98(26), pp. 15131–15136.

Inlay, M.A. *et al.* (2009) 'Ly6d marks the earliest stage of B-cell specification and identifies the branchpoint between B-cell and T-cell development', *Genes & Development*, 23(20), pp. 2376–2381.

Ivanovs, A. *et al.* (2011) 'Highly potent human hematopoietic stem cells first emerge in the intraembryonic aorta-gonad-mesonephros region', *Journal of Experimental Medicine*, 208(12), pp. 2417–2427.

Jameson, S.C., Hogquist, K.A. and Bevan, M.J. (1995) 'Positive selection of thymocytes', *Annual review of immunology*, 13, pp. 93–126.

Jonat, C. *et al.* (1990) 'Antitumor promotion and antiinflammation: Down-modulation of AP-1 (Fos/Jun) activity by glucocorticoid hormone', *Cell*, 62(6), pp. 1189–1204.

Jones, C.A. *et al.* (2020) 'Antenatal corticosteroid administration is associated with decreased growth of the fetal thymus: a prospective cohort study', *Journal of Perinatology*, 40(1), pp. 30–38.

Kajantie, E. *et al.* (2004) 'Circulating Glucocorticoid Bioactivity in the Preterm Newborn after Antenatal Betamethasone Treatment', *The Journal of Clinical Endocrinology & Metabolism*, 89(8), pp. 3999–4003.

Kawa, M.P. *et al.* (2022) 'Apoptosis Evaluation in Circulating CD34+-Enriched Hematopoietic Stem and Progenitor Cells in Patients with Abnormally Increased Production of Endogenous Glucocorticoids in Course of Cushing's Syndrome', *International Journal of Molecular Sciences*, 23(24), p. 15794.

Kenneson, A. and Cannon, M.J. (2007) 'Review and meta-analysis of the epidemiology of congenital cytomegalovirus (CMV) infection', *Reviews in Medical Virology*, 17(4), pp. 253–276.

Klenerman, P. and Oxenius, A. (2016) 'T cell responses to cytomegalovirus.', *Nature reviews. Immunology*, 16(6), pp. 367–77.

Korzhenevich, J. *et al.* (2023) 'Human and mouse early B cell development: So similar but so different.', *Immunology letters*, 261, pp. 1–12.

Kumar, R. and Thompson, E.B. (2005) 'Gene regulation by the glucocorticoid receptor: Structure:function relationship', *The Journal of Steroid Biochemistry and Molecular Biology*, 94(5), pp. 383–394.

Kumaravelu, P. *et al.* (2002) 'Quantitative developmental anatomy of definitive haematopoietic stem cells/long-term repopulating units (HSC/RUs): role of the aorta-gonad-mesonephros (AGM) region and the yolk sac in colonisation of the mouse embryonic liver', *Development*, 129(21), pp. 4891–4899.

Landreth, K.S. (2002) 'Critical windows in development of the rodent immune system', *Human & Experimental Toxicology*, 21(9–10), pp. 493–498.

Larsen, A.D. *et al.* (2014) 'Exposure to psychosocial job strain during pregnancy and odds of asthma and atopic dermatitis among 7-year old children - a prospective cohort study.', *Scandinavian journal of work, environment & health*, 40(6), pp. 639–48.

Lee, A. *et al.* (2016) 'Prenatal and postnatal stress and asthma in children: Temporal- and sex-specific associations', *Journal of Allergy and Clinical Immunology*, 138(3), pp. 740-747.e3.

Lenaerts, A. *et al.* (2022) 'EBF1 primes B-lymphoid enhancers and limits the myeloid bias in murine multipotent progenitors.', *The Journal of experimental medicine*, 219(11).

Liggins, G.C. and Howie, R.N. (1972) 'A controlled trial of antepartum glucocorticoid treatment for prevention of the respiratory distress syndrome in premature infants.', *Pediatrics*, 50(4), pp. 515–25.

Lill-Elghanian, D. *et al.* (2002) 'Glucocorticoid-Induced Apoptosis in Early B Cells from Human Bone Marrow', *Experimental Biology and Medicine*, 227(9), pp. 763–770.

Lorenzo Bermejo, J., Sundquist, J. and Hemminki, K. (2007) 'Risk of Cancer among the Offspring of Women Who Experienced Parental Death during Pregnancy', *Cancer Epidemiology, Biomarkers & Prevention*, 16(11), pp. 2204–2206.

Mattos, G.E. *et al.* (2013) 'Corticosteroid-binding globulin contributes to the neuroendocrine phenotype of mice selected for extremes in stress reactivity', *Journal of Endocrinology*, 219(3), pp. 217–229.

McGoldrick, E. *et al.* (2020) 'Antenatal corticosteroids for accelerating fetal lung maturation for women at risk of preterm birth.', *The Cochrane database of systematic reviews*, 12(12), p. CD004454.

McGrath, K.E. *et al.* (2015) 'Distinct Sources of Hematopoietic Progenitors Emerge before HSCs and Provide Functional Blood Cells in the Mammalian Embryo', *Cell reports*, 11(12), pp. 1892–1904.

Medetgul-Ernar, K. and Davis, M.M. (2022) 'Standing on the shoulders of mice', *Immunity*, 55(8), pp. 1343–1353.

Medvinsky, A. and Dzierzak, E. (1996) 'Definitive Hematopoiesis Is Autonomously Initiated by the AGM Region', *Cell*, 86(6), pp. 897–906.

Melvan, J.N. *et al.* (2010) 'Neonatal Sepsis and Neutrophil Insufficiencies', *International reviews of immunology*, 29(3), p. 315.

Mestas, J. and Hughes, C.C.W. (2004) 'Of Mice and Not Men: Differences between Mouse and Human Immunology', *The Journal of Immunology*, 172(5), pp. 2731–2738.

Michie, C.A., Hasson, N. and Tulloh, R. (1998) 'The neonatal thymus and antenatal steroids.', *Archives of disease in childhood. Fetal and neonatal edition*, 79(2), p. F159.

Miller, J.F.A.P. (2011) 'The golden anniversary of the thymus.', *Nature reviews. Immunology*, 11(7), pp. 489–95.

Mittelstadt, P.R., Taves, M.D. and Ashwell, J.D. (2018) 'Cutting Edge: De Novo Glucocorticoid Synthesis by Thymic Epithelial Cells Regulates Antigen-Specific Thymocyte Selection', *The Journal of Immunology*, 200(6), pp. 1988–1994.

Müller, A.M. *et al.* (1994) 'Development of hematopoietic stem cell activity in the mouse embryo', *Immunity*, 1(4), pp. 291–301.

Nagasawa, H., Miyamoto, M. and Fujimoto, M. (1973) 'Reproductivity in Inbred Strains of Mice and Project for Their Efficient Production', *Experimental Animals*, 22(2), pp. 119–126.

Nagase, H. *et al.* (2000) 'Glucocorticoids preferentially upregulate functional CXCR4 expression in eosinophils', *The Journal of allergy and clinical immunology*, 106(6), pp. 1132–1139.

Nemazee, D. (2017) 'Mechanisms of central tolerance for B cells', *Nature Reviews Immunology*, 17(5), pp. 281–294.

Ninan, K. *et al.* (2023) 'The proportions of term or late preterm births after exposure to early antenatal corticosteroids, and outcomes: systematic review and meta-analysis of 1.6 million infants.', *BMJ (Clinical research ed.)*, 382, p. e076035.

Nutt, S.L. and Kee, B.L. (2007) 'The Transcriptional Regulation of B Cell Lineage Commitment', *Immunity*, 26(6), pp. 715–725.

Oppong, E. and Cato, A.C.B. (2015) 'Effects of glucocorticoids in the immune system', *Advances in Experimental Medicine and Biology*, 872, pp. 217–233.

Osterholm, E.A. and Schleiss, M.R. (2020) 'Impact of breast milk-acquired cytomegalovirus infection in premature infants: Pathogenesis, prevention, and clinical consequences?', *Reviews in Medical Virology*. John Wiley and Sons Ltd, pp. 1–11.

Palis, J. *et al.* (1999) 'Development of erythroid and myeloid progenitors in the yolk sac and embryo proper of the mouse', *Development*, 126(22), pp. 5073–5084.

Palis, J. (2014) 'Primitive and definitive erythropoiesis in mammals', *Frontiers in Physiology*, 5, 3.

Palmer, E. (2003) 'Negative selection--clearing out the bad apples from the T-cell repertoire', *Nature reviews. Immunology*, 3(5), pp. 383–391.

Palmetti, M. *et al.* (2025) 'Congenital CMV infection and central nervous system involvement: mechanisms, treatment, and long-term outcomes', *European Journal of Pediatrics*, 184(6), p. 381.

Perin, H.J. *et al.* (2022) 'Global, regional, and national causes of under-5 mortality in 2000-19: an updated systematic analysis with implications for the Sustainable Development Goals', *Lancet Child Adolesc Health*, 6, pp. 106–121.

Perna-Barrull, D. *et al.* (2019) 'Prenatal Betamethasone interferes with immune system development and alters target cells in autoimmune diabetes', *Scientific Reports*, 9(1), p. 1235.

Perna-Barrull, D. *et al.* (2020) 'Immune System Remodelling by Prenatal Betamethasone: Effects on β-Cells and Type 1 Diabetes', *Frontiers in Endocrinology*, 11.

Perna-Barrull, D. *et al.* (2023) 'Impact of Betamethasone Pretreatment on Engrafment of Cord Blood-Derived Hematopoietic Stem Cells', *Archivum Immunologiae et Therapiae Experimentalis*, 71(1), p. 1.

Pole, J.D. *et al.* (2009) 'Antenatal steroid therapy for fetal lung maturation: Is there an association with childhood asthma?', *Journal of Asthma*, 46(1), pp. 47–52.

Preidis, G.A. *et al.* (2011) 'Pneumonia and Malnutrition are Highly Predictive of Mortality among African Children Hospitalized with Human Immunodeficiency Virus Infection or Exposure in the Era of Antiretroviral Therapy', *The Journal of Pediatrics*, 159(3), pp. 484–489.

Räikkönen, K. *et al.* (2023) 'Antenatal corticosteroid treatment and infectious diseases in children: a nationwide observational study', *The Lancet Regional Health - Europe*, 35, p. 100750.

Raymond, J. and Aujard, Y. (2000) 'Nosocomial infections in pediatric patients: a European, multicenter prospective study. European Study Group', *Infection control and hospital epidemiology*, 21(4), pp. 260–263.

Rieger, M.A. and Schroeder, T. (2012) 'Hematopoiesis', *Cold Spring Harbor Perspectives in Biology*, 4(12), pp. a008250–a008250.

Robson MacDonald, H., Wilson, A. and Radtke, F. (2001) 'Notch1 and T-cell development: insights from conditional knockout mice', *Trends in Immunology*, 22(3), pp. 155–160.

Scheinman, R.I. *et al.* (1995) 'Characterization of mechanisms involved in transrepression of NF-kappa B by activated glucocorticoid receptors.', *Molecular and cellular biology*, 15(2), pp. 943–53.

Schmitt, T.M. *et al.* (2004) 'Maintenance of T Cell Specification and Differentiation Requires Recurrent Notch Receptor–Ligand Interactions', *The Journal of Experimental Medicine*, 200(4), pp. 469–479.

Shah, B.A. and Padbury, J.F. (2014) 'Neonatal sepsis', *Virulence*, 5(1), pp. 170–178.

Shimizu, Y. *et al.* (2023) 'Influence of Immune System Abnormalities Caused by Maternal Immune Activation in the Postnatal Period', *Cells*, 12(5), p. 741.

Soares-da-Silva, F. *et al.* (2020) 'Crosstalk Between the Hepatic and Hematopoietic Systems During Embryonic Development', *Frontiers in Cell and Developmental Biology*, 8, p. 612.

Soares-da-Silva, F. *et al.* (2023) 'Assembling the layers of the hematopoietic system: A window of opportunity for thymopoiesis in the embryo', *Immunological Reviews*, 315(1), pp. 54–70.

Solano, M.E. *et al.* (2016) 'Antenatal endogenous and exogenous glucocorticoids and their impact on immune ontogeny and long-term immunity', *Seminars in Immunopathology*, 38(6), pp. 739–763.

Souabni, A. *et al.* (2002) 'Pax5 Promotes B Lymphopoiesis and Blocks T Cell Development by Repressing Notch1', *Immunity*, 17(6), pp. 781–793.

Stahl, F.R. *et al.* (2013) 'Nodular Inflammatory Foci Are Sites of T Cell Priming and Control of Murine Cytomegalovirus Infection in the Neonatal Lung', *PLoS Pathogens*, 9(12), p. e1003828.

Stein, R.T. *et al.* (2017) 'Respiratory Syncytial Virus Hospitalization and Mortality: Systematic Review and Meta-Analysis', *Pediatric Pulmonology*, 52, pp. 556–569.

Swanson, M.R. *et al.* (2025) 'Beyond hearing loss: exploring neurological and neurodevelopmental sequelae in asymptomatic congenital cytomegalovirus infection', *Pediatric Research*, 10.1038/s41390-025-04232-5.

Tabone, M.D. *et al.* (2000) 'Nosocomial infections in immunocompromised children.', *Pathologie-biologie*, 48(10), pp. 893–900.

Tagoh, H. *et al.* (2006) 'The mechanism of repression of the myeloid-specific c-fms gene by Pax5 during B lineage restriction', *EMBO Journal*, 25(5), pp. 1070–1080.

Taves, M.D. and Ashwell, J.D. (2021) 'Glucocorticoids in T cell development, differentiation and function', *Nature Reviews Immunology*, 21(4), pp. 233–243.

Tolosa, E., King, L.B. and Ashwell, J.D. (1998) 'Thymocyte Glucocorticoid Resistance Alters Positive Selection and Inhibits Autoimmunity and Lymphoproliferative Disease in MRL-Mice', *Immunity*, 8(1), pp. 67–76.

Tsapogas, P. *et al.* (2017) 'The Cytokine Flt3-Ligand in Normal and Malignant Hematopoiesis', *International Journal of Molecular Sciences*, 18(6), p. 1115.

Tseng, W.-N. *et al.* (2016) 'Antenatal Dexamethasone Exposure in Preterm Infants Is Associated with Allergic Diseases and the Mental Development Index in Children', *International Journal of Environmental Research and Public Health*, 13(12), p. 1206.

Ugor, E. *et al.* (2018) 'Glucocorticoid hormone treatment enhances the cytokine production of regulatory T cells by upregulation of Foxp3 expression', *Immunobiology*, 223(4–5), pp. 422–431.

Vacchio, M.S., Papadopoulos, V. and Ashwell, J.D. (1994) 'Steroid production in the thymus: implications for thymocyte selection', *The Journal of experimental medicine*, 179(6), pp. 1835–1846.

Vermillion, S.T., Soper, D.E. and Newman, R.B. (2000) 'Neonatal sepsis and death after multiple courses of antenatal betamethasone therapy', *American journal of obstetrics and gynecology*, 183(4), pp. 810–814.

Wang, L. *et al.* (2015) 'Glucocorticoids induce autophagy in rat bone marrow mesenchymal stem cells', *Molecular Medicine Reports*, 11(4), pp. 2711–2716.

Weber, P.S.D. *et al.* (2004) 'Mechanisms of glucocorticoid-induced down-regulation of neutrophil L-selectin in cattle: evidence for effects at the gene-expression level and primarily on blood neutrophils', *Journal of Leukocyte Biology*, 75(5), pp. 815–827.

Wen, H. *et al.* (2011) 'Prediction of atopic dermatitis in 2-yr-old children by cord blood IgE, genetic polymorphisms in cytokine genes, and maternal mentality during pregnancy', *Pediatric Allergy and Immunology*, 22(7), pp. 695–703.

World Health Organization (2022) 'WHO recommendations on Antenatal corticosteroids for improving preterm birth outcomes', *WHO recommendations on: Antenatal corticosteroids for improving preterm birth outcomes*, pp. 9-14.

Wyllie, A.H. (1980) 'Glucocorticoid-induced thymocyte apoptosis is associated with endogenous endonuclease activation', *Nature*, 284(5756), pp. 555–556.

Yao, T.C. *et al.* (2023) 'Association between antenatal corticosteroids and risk of serious infection in children: nationwide cohort study', *BMJ (Clinical research ed.)*, 382, p. e075835.

Zaoutis, T.E. *et al.* (2006) 'Epidemiology, Outcomes, and Costs of Invasive Aspergillosis in Immunocompromised Children in the United States, 2000', *Pediatrics*, 117(4), pp. e711–e716.

Zhang, X., Zhivaki, D. and Lo-Man, R. (2017) 'Unique aspects of the perinatal immune system', *Nature Reviews Immunology*, 17(8), pp. 495–507.

Zook, E.C. and Kee, B.L. (2016) 'Development of innate lymphoid cells', *Nature Immunology*, 17(7), pp. 775–782.

Zúñiga-Pflücker, J.C. (2004) 'T-cell development made simple', *Nature Reviews Immunology*, 4(1), pp. 67–72.

9. Abbreviations

ACS	Antenatal corticosteroid
AGM	aorta-gonad-mesonephros region
ARDS	Acute respiratory distress syndrome
BCR	B cell receptor
BLP	B cell-committed lymphoid progenitor cell
CBMC	cord blood mononuclear cell
cCMV	congenital cytomegalovirus
CD4 SP	$CD4^+$ single positive T cell
CD8 SP	$CD8^+$ single positive T cell
C/EBPα	CCAAT/Enhancer Binding protein α
CDP	Comon dendritic cell progenitor
CLP	Common lymphoid progenitor cell
CMJ	Corticomedullary junction
CMP	Common myeloid progenitor cell
CMV	Cytomegalovirus
DN	Double negative ($CD4^-$ $CD8^-$) thymocyte
DP	Double positive ($CD4^+$ $CD8^+$) thymocyte
E	embryonic day
ETP	early thymic progenitor
GC	Glucocorticoid
GM-CSF	Granulocyte-macrophage colony-stimulating factor
GMP	Granulocyte-macrophage-progenitor
HCMV	Human cytomegalovirus
HSC	Hematopoietic stem cell
HSPC	Hematopoietic stem and progenitor cell
ISP8	intermediate CD8 single positive thymocyte
LMPP	Lymphoid-primed multipotent progenitor cell
LSK	Pluripotent Lin-, Sca1+, cKit+ cell
MCMV	Murine cytomegalovirus
MDP	Monocyte-dendritic cell progenitor
MEP	Megakaryocyte-erythrocyte-progenitor cell

MPP	Multipotent progenitor cell
mTEC	Medullary thymic epithelial cell
NK cell	Natural killer cell
PAX5	paired box 5
PBMC	Peripheral blood mononuclear cell
PBS	Phosphate-buffered saline
PCW	Postconceptual week
PND	Postnatal day
RAG	Recombination-activating gene
SCF	Stem cell factor
TF	Transcription factor
TLP	T-cell committed lymphoid progenitor cell
TSP	Thymus-seeding progenitor
YS	Yolk sac

10. List of Figures

Supplementary Figures (Appendix)

11. List of Tables

12. Appendix

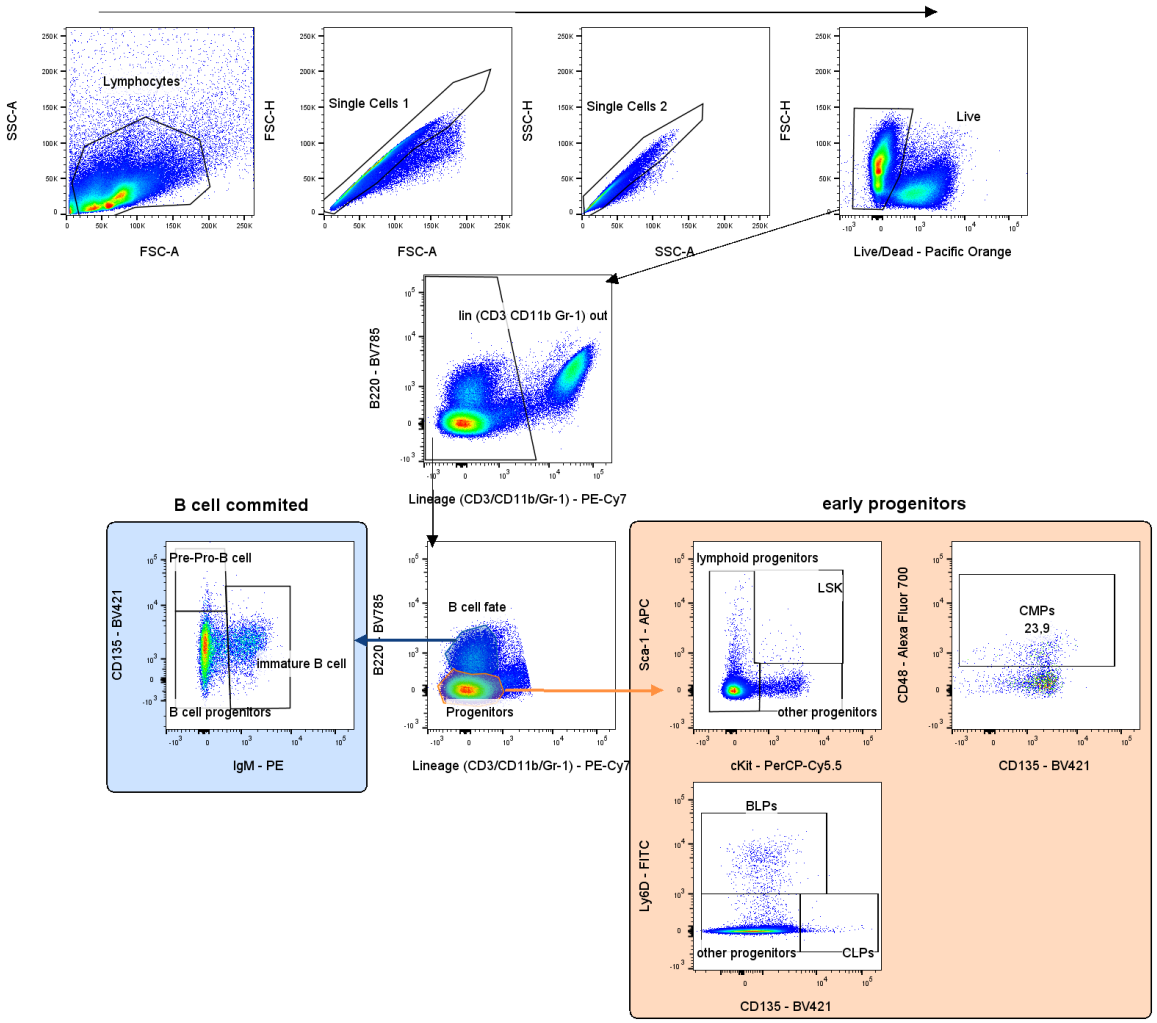

Figure S1: Gating strategy for progenitor cells in bone marrow (Panel 1). Gating strategy for a 10-color flow cytometry analysis of leukocytes from bone marrow. Representative sample of a 3-day old PBS treated C57BL/6 WT mouse.

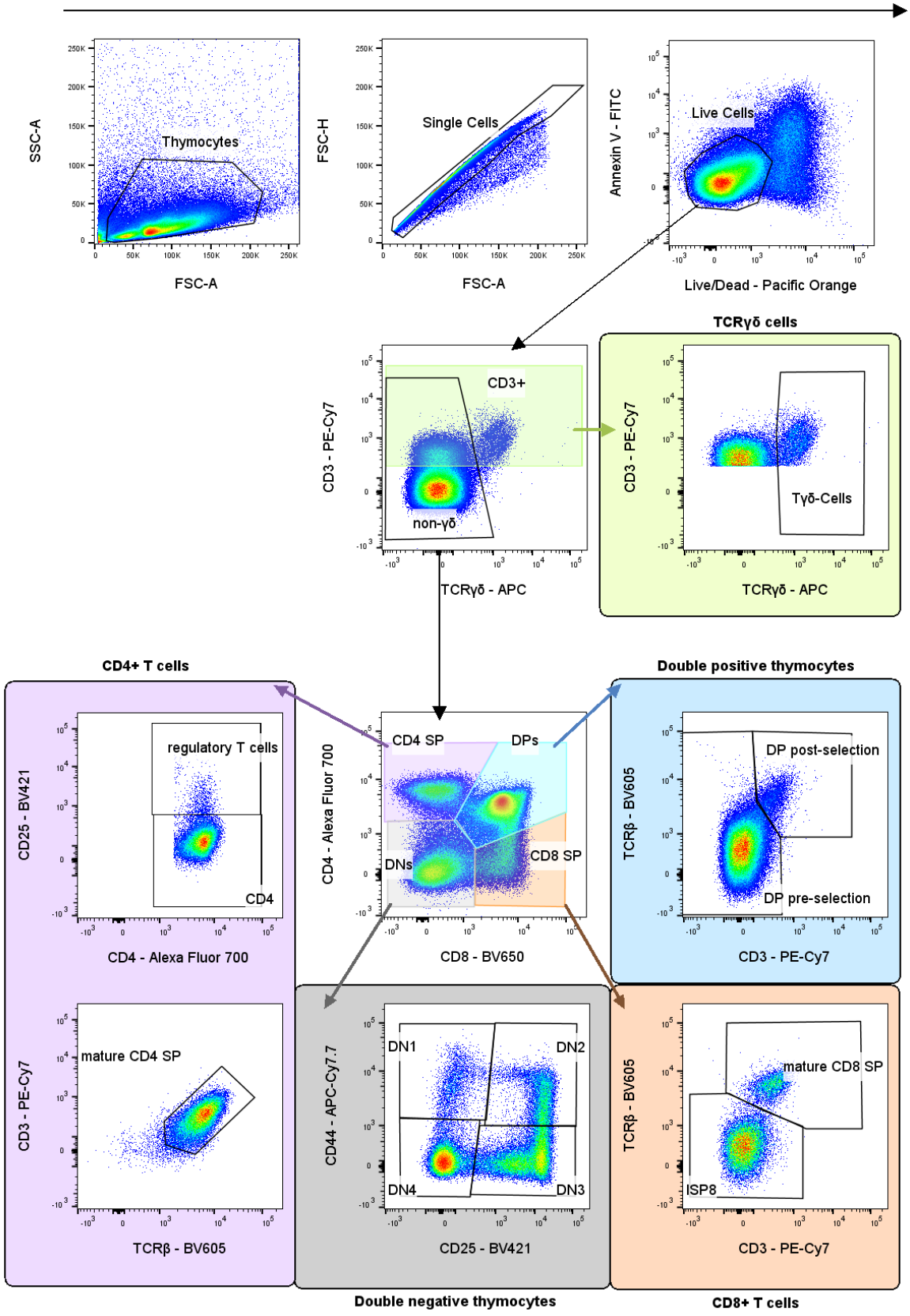

Figure S2: Gating strategy for T-cell development panel in thymus (Panel 2). Gating strategy for a 12-color flow cytometry analysis of leukocytes from thymus. Representative plot of a 3-day old PBS treated C57BL/6 WT mouse.

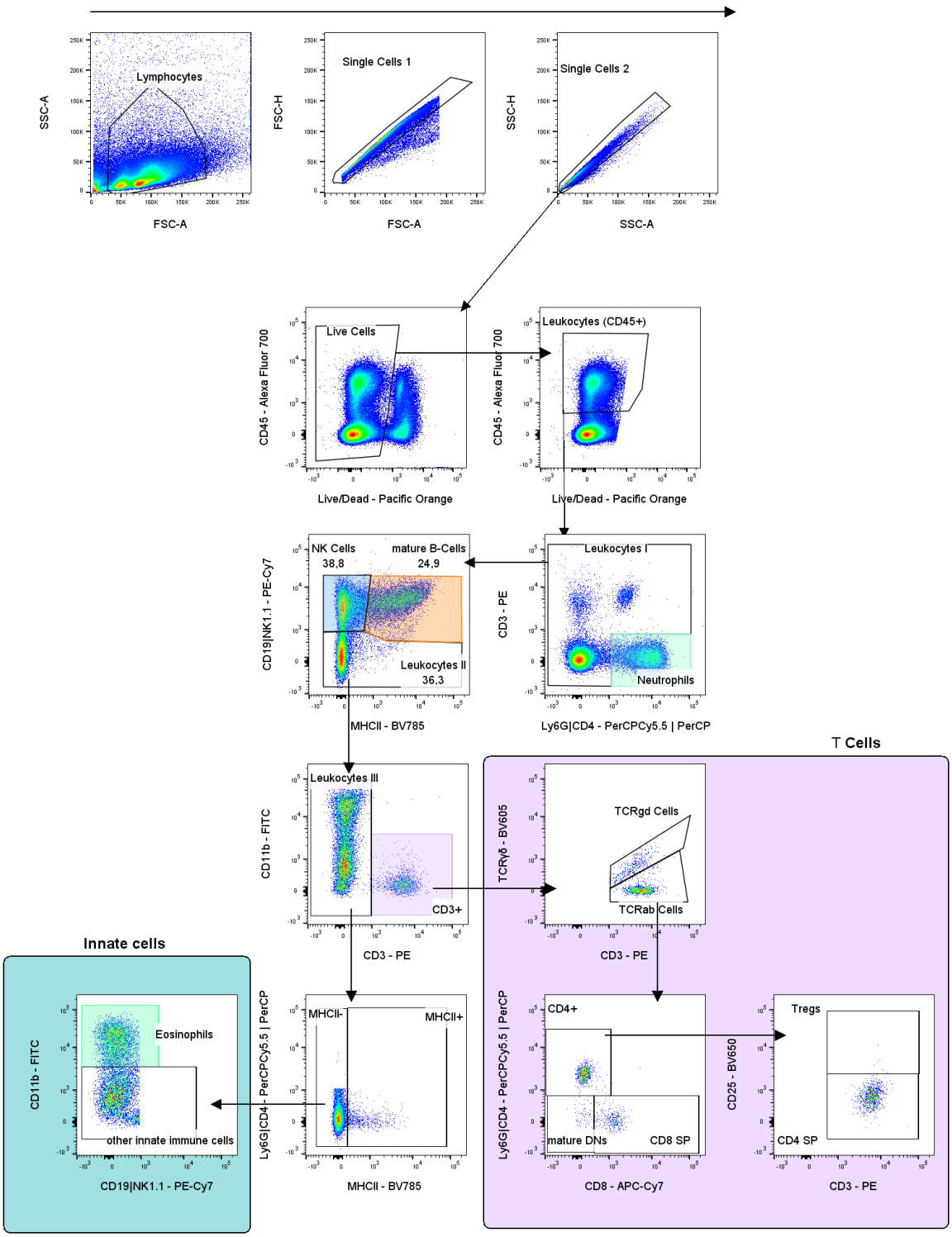

Figure S3: Gating strategy for immune cell populations in spleen and blood (Panel 3). Gating strategy for a 15-color flow cytometry analysis of leukocytes from spleen and blood. Representative plot from spleen of a 3-day old PBS treated C57BL/6 WT mouse.

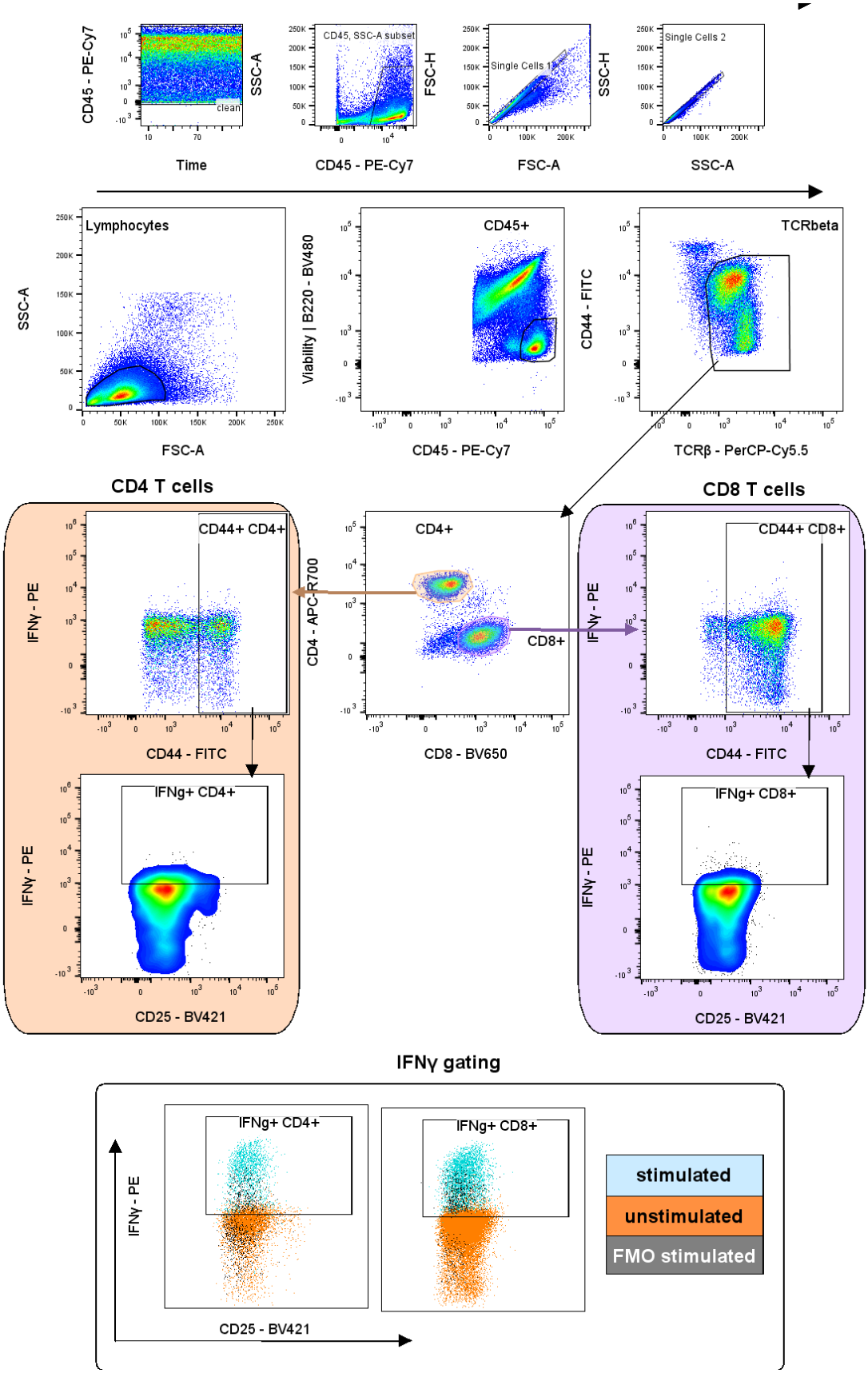

Figure S4: Gating strategy for CD8 T cells and IFNγ production in spleen (Panel 4). Gating strategy for a 12-color flow cytometry analysis of leukocytes from spleen. Representative plot from spleen of a 3-day old PBS treated C57BL/6 WT mouse.

13. List of Publications

Bremer SJ, Boxnick A, Glau L, Biermann D, Joosse SA, Thiele F, **Billeb E**, May J, Kolster M, Hackbusch R, Fortmann MI, Kozlik-Feldmann R, Hübler M, Tolosa E, Sachweh JS, Gieras A. Thymic Atrophy and Immune Dysregulation in Infants with Complex Congenital Heart Disease. J Clin Immunol. 2024 Feb 23;44(3):69.

14. Contribution statement

The work for this thesis was carried out in the Institute for Immunology at the University Medical Center Hamburg-Eppendorf under the supervision of Prof. Eva Tolosa. The study was designed by Prof. Dr. Eva Tolosa and Dr. Anna Gieras.

The following sections of this thesis are based on my direct (collaborative) work:

- Experimental and flow-cytometry panel design: Under supervision of Prof. Dr. Eva Tolosa and Dr. Anna Gieras
- Mouse breeding and animal scoring: Together with the laboratory animal husbandry of the UKE
- Prenatal betamethasone application
- Organ harvesting for the peripheral seeding project
- Organ harvesting for the MCMV infection project: Together with S. Tödter
- Single cell suspension and FACS-staining
- Immune cell stimulation
- Flow-cytometry measurements
- Statistical and data analysis: Under supervision of Prof. Dr. E. Tolosa and Dr. A. Gieras
- Generation of introduction figures and graphical abstract in BioRender

The following parts of the work were not carried out by me. However, I was involved in their evaluation and interpretation:

- Neonatal MCMV infection: S. Tödter
- Luciferase assays: S. Tödter and L. Fonseca Brito

Figures 1, 2, 3, 4, 5 and 6 were created by me using BioRender: Scientific Image and Illustration Software.

ChatGPT (chat.openai.com) was used to check spelling and grammar on the first draft of Aims and Introduction. I guarantee that I carefully checked and adjusted the output of the AI tool before including text in the manuscript.

15. Eidesstattliche Versicherung

Ich versichere ausdrücklich, dass ich die Arbeit selbständig und ohne fremde Hilfe, insbesondere ohne entgeltliche Hilfe von Vermittlungs- und Beratungsdiensten, verfasst, andere als die von mir angegebenen Quellen und Hilfsmittel nicht benutzt und die aus den benutzten Werken wörtlich oder inhaltlich entnommenen Stellen einzeln nach Ausgabe (Auflage und Jahr des Erscheinens), Band und Seite des benutzten Werkes kenntlich gemacht habe. Das gilt insbesondere auch für alle Informationen aus Internetquellen.
Soweit beim Verfassen der Dissertation KI-basierte Tools („Chatbots“) verwendet wurden, versichere ich ausdrücklich, den daraus generierten Anteil deutlich kenntlich gemacht zu haben. Die „Stellungnahme des Präsidiums der Deutschen Forschungsgemeinschaft (DFG) zum Einfluss generativer Modelle für die Text- und Bilderstellung auf die Wissenschaften und das Förderhandeln der DFG“ aus September 2023 wurde dabei beachtet.
Ferner versichere ich, dass ich die Dissertation bisher nicht einem Fachvertreter an einer anderen Hochschule zur Überprüfung vorgelegt oder mich anderweitig um Zulassung zur Promotion beworben habe.
Ich erkläre mich damit einverstanden, dass meine Dissertation vom Dekanat der Medizinischen Fakultät mit einer gängigen Software zur Erkennung von Plagiaten überprüft werden kann.

Datum Unterschrift

16. Acknowledgments

I would like to express my deepest appreciation and gratitude to my supervisor Prof. Dr. Eva Tolosa for her constant support, everlasting patience, knowledge and expertise shared with me throughout every step of the way and also beyond the lab. My deepest thanks go to my supervisor Dr. Anna Gieras for her guidance and the constructive feedback during the last years.

Special thanks to the entire Tolosa lab for a time of learning, adventure and inspiration. Laura, Enja, Riekje, Jolan, Tina, Anne, Manu, Romy, Dana, Hauke, Hanna, Annika and Kati - the memories with you will forever be treasured. I am especially grateful to Manuela Kolster and Romy Hackbusch for showing me the ways of the lab and for their excellent technical help.

Many thanks to Prof. Dr. Felix Stahl for being my external committee supervisor and to him, Silvia Tödter and Dr. Luís Fonseca Brito for the productive collaboration on the MCMV infection project.

I thank Sabrina Noster for her animal husbandry.

I thank the iPRIME graduate school for financial support, the informative seminars, and enabling productive networking.

Finally, I would like to thank my parents for the trust and support throughout the years and to my friends and my partner for their never-ending patience, emotional support, pep talks and for cooking for me when I forgot.